Synthesis, molecular structure, conformational, and intramolecular hydrogen bond strength of ethyl 3-amino-2-butenoate and its N-Me, N-Ph, and N-Bn analogs; an experimental and theoretical study

Bazrafshan, Mahmoud; Vakili, Mohammad; Tayyari , Sayyed Faramarz ; Kamounah, Fadhil S. ; Hansen, Poul Erik; Shiri, Ali

Published in:
Journal of Molecular Structure

DOI:
10.1016/j.molstruc.2022.134479

Publication date:
2023

Document Version
Early version, also known as pre-print

Citation for published version (APA):
Bazrafshan, M., Vakili, M., Tayyari , S. F., Kamounah, F. S., Hansen, P. E., & Shiri, A. (2023). Synthesis, molecular structure, conformational, and intramolecular hydrogen bond strength of ethyl 3-amino-2-butenoate and its N-Me, N-Ph, and N-Bn analogs; an experimental and theoretical study. *Journal of Molecular Structure*, *1274*(Part 2), Article 134479. https://doi.org/10.1016/j.molstruc.2022.134479

Synthesis, molecular structure, conformational, and intramolecular hydrogen bond strength of ethyl 3-amino-2-butenoate and its N-Me, N-Ph, and N-Bn analogs; an experimental and theoretical study

Mahmoud Bazrafshan [a], Mohammad Vakili [a]*, Sayyed Faramarz Tayyari [a], Fadhil S. Kamounah [b], Poul Erik Hansen [c], Ali Shiri [a]

[a] *Department of Chemistry, Faculty of Science, Ferdowsi University of Mashhad, Mashhad, Iran*

[b] *Department of Chemistry, University of Copenhagen, Universitetsparken 5, DK-2100, Copenhagen Ø, Denmark*

[c] *Department of Science and Environment, Roskilde University, Universitetsvej 1, P.O. Box 260, DK-4000, Roskilde, Denmark*

Corresponding author

* vakili-m@um.ac.ir (Mohammad Vakili)

Tel/Fax: +989153215410

Abstract

Amino derivatives of ethyl acetoacetate like ethyl (Z)- 3-(amino)but-2-enoate (EAB), ethyl (Z)- 3-(methylamino)but-2-enoate (Me-EAB), ethyl (Z)- 3-(phenylamino)but-2-enoate (Ph-EAB), and ethyl (Z)- 3-(benzylamino)but-2-enoate (Bn-EAB) were synthesized. Their structures, conformations, and intramolecular hydrogen bonding (IHB) is characterized using computational analysis (density functional theory, DFT, methods) at the B3LYP/6-311++G(d,p) level and spectroscopic techniques (IR, UV, and NMR). All the mentioned theoretical and experimental

results were compared to those of (Z)-methyl 3-aminobut-2-enoate (MAB). The vibrational spectra of EAB are fully assigned. Vibrational spectroscopy results confirmed the existence of two conformers of title molecules. DFT calculations at the B3LYP/6-311++G(d,p) level show the calculated N-H bond lengths in EAB, Me-EAB, Ph-EAB, Bn-EAB, and MAB are 1.015, 1.017, 1.022, 1.018, and 1.014 Å, respectively. Also, according to the natural bond orbital (NBO) results, the σN-H10↔LP(2)O7 interactions for EAB, Me-EAB, Ph-EAB, Bn-EAB, and MAB are 5.21, 6.77, 8.65, 7.18, and 5.11 kcal/mol, respectively. So, the trend in IHB strength is: Ph-EAB > Bn-EAB ~ Me-EAB > EAB ~ MAB, which also agrees with the mentioned experimental results. The mentioned trend also is confirmed by the LP(O7)↔σN-H steric exchange interaction.

Keywords: Ethyl (Z)- 3-(amino)but-2-enoate; Intramolecular hydrogen bond; NMR; Vibrational spectroscopy; DFT.

1. Introduction

β-enamino esters, with N–C=C–C=O skeleton, are used to prepare bio-active heterocyclic compounds such as pyridinone, tetronic acids, pyrazoles, quinolines, and oxazoles [1-4]. They have been used to prepare antitumor agents [5], anticonvulsant [6], anti-inflammatory [7], and antibacterial [8]. They are also important precursors for the synthesis of indolizidine alkaloids [9], azo compounds [10], 3-amino sugar derivatives [11], hexahydro azulenes [12], and β-amino ketones [13]. Theoretically, β-enamino esters can form three different tautomers including iminoenol, iminoketone, and aminoketone forms (see Fig. 1). The present study will elucidate the possible existence of all three. Examples of enaminones are many, but the resemblance between those and enaminoesters is slight due to the difficulty of esters to exist as enol forms. Nevertheless, a product in the iminoenol form has been postulated [14] (see Discussion).

<Fig. 1>

One of the most simple members of the β-enamino esters is MAB, which is used as a reference in this work. MAB's vibrational spectra, structure, and hydrogen bond strength have been studied experimentally and theoretically [15]. Recently, Singh et al. [16] synthesized EAB and a

few of its N-substituted derivatives to make 5-hydroxyindoles via scaffolds based on a Nenitzescu reaction, but the structure, conformation, and full interpretation of the vibrational bands in EAB and N-methyl, phenyl, and benzyl substitutions have not been reported. The above substitutions can affect the strength of the hydrogen bond by steric and electronic effects. Comparing the strength of the hydrogen bond with experimental and theoretical methods, such as NMR, UV-Vis, IR, Raman spectra, optimized geometric parameters, NBO, and atoms in molecules (AIM) [17] analysis, of the investigated molecules with MAB [15], can increase our insight into the effects of these substitutions on the strength of IHB.

2. Experimental

2.1. Materials and measurements

Unless stated otherwise, all chemicals were purchased from Sigma-Aldrich and used without further purification. Solvents used were HPLC grade and dried over molecular sieves (4 Å) before use. Analytical thin-layer chromatography was done on Merck Alufoils SiO_2 60 F254 0.2 mm thick precoated TLC plates. Column chromatography was performed using SiO_2 from VWR 40−63 μm. ^{1}H and ^{13}CNMR spectra were also recorded at 500 and 126 MHz, respectively, on a Bruker Avance 3 spectrometer with a BBFO probe. All chemical shifts (δ) are quoted in ppm, and all coupling constants (J) are in Hertz (Hz). The following abbreviations are used for diversity for NMR resonances: s=singlet, bs=broad singlet, d=doublet, t=triplet, q=quartet, and m=multiplet. HRMS LC/MS were recorded on a Dionex Acclaim RSLC 120 C18 2.2 lm 120 Å 2.150 mm column maintained at 40 ˚C carried out on a Bruker Micro TOF-QII system with ESI system.

The mid-IR spectra were obtained using KBr pellets or CCl_4 solution with a spectral resolution of 2 cm^{-1} by averaging the results of 20 scans with a Bomem MB-154 Fourier transform spectrophotometer.

The FT-Raman spectrum of EAB was recorded on a Teksan, Takram P50C0R10 Raman spectrophotometer with 532 nm wavelength incident laser light.

The Far-IR spectra in the region 600-200 cm^{-1} were obtained using a Thermo Nicolet NEXUS 870 FT-IR spectrometer equipped with a DTGS/polyethylene detector and a solid substrate beam splitter with the use of polyethylene disks. The spectrum was collected using CsI pellets with a resolution of 2 cm^{-1} by signal averaging 32 scans.

The deuterated analog of EAB, D_3-EAB, was prepared according to the literature [18]. According to the IR spectra, the hydrogen atoms of the amino group and α-position were replaced by deuterium.

The ultraviolet absorption spectra were examined in the 200–400 nm range using Perkin-Elmer LAMBDA 25 spectrophotometer equipped with a 10 mm quartz cell at 298 K. Ethanol was used as a solvent in the UV study.

2.2. Synthesis

The synthesis of ethyl (Z)-3-(methylamino)but-2-enoate, Me-EAB, and ethyl (Z)- 3-(phenylamino)but-2-enoate, Ph-EAB, was recently reported [19]. Ethyl (Z)- 3-(amino)but-2-enoate (EAB) and ethyl (Z)- 3-(benzylamino)but-2-enoate (Bn-EAB) were synthesized using the following protocols.

(Z)- 3-(amino)but-2-enoate, EAB:

In 100 ml, RBF was charged with ethyl acetoacetate (2.08 g, 16.0 mmol) and ammonium acetate (6.13 g, 80.0 mmol) in methanol (25 ml). The flask was stoppered, and the mixture was stirred at room temperature for 48 h. Then more ammonium acetate (2.03 g, 26.4 mmol) was added, and the mixture was stirred at room temperature for another 24 h. After the solvent was evaporated under reduced pressure, the residue was diluted with chloroform (60 ml). The resulting solid was filtered off and washed with chloroform (2 × 30 ml). The combined filtrate was washed with water, 1 M KH_2PO_4 solution, brine, and dried with anhydrous sodium sulfate. Evaporation of the solvent gave a white solid purified by flash column chromatography on silica gel, using n-hexane-ethyl acetate (3:2) as eluent to give the pure compound as a light amber oil which solidified on standing (1.58 g, 76%). ^{1}H NMR (500 MHz, $CDCl_3$): δ 7.88 (bs, -NH, 1H), 4.50 (s, 2H), 4.08 (q, 2H, *J*= 7.1 Hz), 1.88 (s, -CH_3, 3H), 1.23 (t, *J*= 7.1 Hz, 3H). ^{13}C NMR (126 MHz, $CDCl_3$): δ 170.36, 159.77, 84.24, 56.61, 22.42, 14.68. HRMS-ESP (m/z): $[M + H]^+$ calcd. For $C_6H_{12}NO_2$: 130.08680, found: 130.0874.

(Z)- 3-(benzylamino)but-2-enoate , Bn-EAB:

In 25 ml, RBF was charged with ethyl acetoacetate (1.30 g, 10.0 mmol), benzyl amine (1.07 g, 10.0 mmol), and glacial acetic acid (0.06 g, 1.0 mmol). The flask was stoppered and shaken in an ultrasound bath at 25 ºC for 1.0 h. The reaction was monitored by TLC and showed complete conversion. The acetic acid was removed under reduced pressure, the amber oil residue was dissolved in dichloromethane (75 ml), washed with water (3x75 ml), and the organic portion was dried over anhydrous sodium sulfate. Evaporation of solvent affords light brown viscous oil purified by flash column chromatography on silica gel, using n-hexane-ethyl acetate (5:1) as eluent to give the pure compound as a light amber oil which solidified on standing (1.49 g, 68%). ^{1}H NMR (500 MHz, $CDCl_3$): δ 8.95 (bs, 1H9), 7.34-7.31 (m, 2H), 7.26-7.23 (m, 3H), 4.53 (s, 1H), 4.41 (d, *J*= 6.4 Hz, 2H), 4.10 (q, *J*= 7.1 Hz, 2H), 1.90 (s, 3H), 1.25 (t, *J*= 7.1 Hz, 3H). ^{13}C NMR (126 MHz, $CDCl_3$): δ 170.92, 162.14, 139.08, 129.10, 127.65, 127.03, 83.51, 58.72, 47.11, 19.70, 14.96, these results are in agreement with literature [16] report. HRMS-ESP (m/z): $[M + H]^+$ calcd. For $C_{13}H_{17}NO_2$: 220.13314, found: 220.13323.

3. Calculations

The calculations for the EAB, Me-EAB, Ph-EAB, and Bn-EAB have been done using the B3LYP functional [20, 21] and the 6-311++G(d,p) basis set using the Gaussian 09W program package [22]. The vibrational assignments of the normal modes are carried out with the GaussView 5.0 software [23]. In addition, the structure's optimization and conformational analysis have also been done at the MP2/6-311++G(d,p) level of theory [24, 25].

The AIM computations were applied according to Bader's AIM theory [17] using the AIM 2000 program [26]. The second-order interaction energies (E^2) [27] and steric exchange energies [28] were calculated using the NBO 5.0 program [29] at MP2/6-311++G(d,p) level of theory.The excitation transitions for the title molecules were calculated by time-dependent density functional theory (TD-DFT), using the polarizable continuum model (PCM) in ethanol as solvent [30]. The GIAO (Gauge-Including Atomic Orbital) method [31, 32] was used to calculate NMR chemical shifts. All the mentioned results were obtained at B3LYP/6-311++G(d,p) level.

4. Results and Discussion

4.1. Molecular structure and intramolecular hydrogen bond strength

As mentioned in the introduction, the EAB and its N-Me, N-Ph, and N-Bn derivatives can, in principle, exist in three different forms called iminoenol (IE), aminoketone (AK), and iminoketone (IK) (see Fig. 1). According to the calculated results, the IE tautomer in EAB is unstable and is changed to AK forms upon optimization. Also, the IK forms, which have no intramolecular hydrogen bond are between 4.3-8.8 kcal/mol higher in energy than AK1. So, the calculated results agree with the experimental and theoretical reported works that showed that the iminoketone and iminoenol tautomers are not stable [15, 33-35]. Also, the recorded NMR and IR spectra confirmed the mentioned results (see continue). So, we consider only AK forms. Only four AK conformers (AK1-AK4) have the N-H···O intramolecular hydrogen bond. AK1-AK4 forms are obtained by varying the C-O-C-C and O=C-O-C dihedral angles (see Fig S1 for EAB, supplementary material). According to the calculations at the B3LYP and MP2 levels with a 6-311++G(d,p) basis set, the AK1 is the most stable conformer, and AK3 and AK4 are the least ones. It agrees for N-Me, N-Ph, and N-Bn derivatives, too. The optimized structures for EAB, AK1, and AK2, with numbering, are shown in Fig. 2. The conformations of the ethoxy group with respect to the chelate ring, Ak1-Ak4, were obtained according to the reported work by Tayyari et al. [33].

<Fig. 2>

The iminoenol form of Bn-EAB has been introduced in the work of Harrad et al. [14]. The proton transfer barrier from AK1 to corresponding IE has been calculated to investigate this further. The relative energy profile for the proton transfer process from the N atom to the O atom (aminoketone form change to iminoenol form) for EAB, calculated at the B3LYP/6-311++G(d,p) level, is shown in Fig. 3a. The activation energy required for the proton transfer process is 15.61 kcal/mol in the gas phase. In Fig. 3b, a similar profile is calculated for Bn-EAB. These two plots demonstrate no transition barrier between the iminoenol and aminoketone forms, indicating that the iminoenol form can not exist. Furthermore, the NMR data in Ref. [14] do not correspond to the iminoenol form.

<Fig. 3>

The most stable conformers of EAB, Me-EAB, Ph-EAB, and Bn-EAB (AK1 and AK2) are shown in Figs. 2 and S2 (see supplementary material). The conformation of OC_2H_5 in Me-EAB, Ph-EAB, and Bn-EAB in the mentioned stable forms is similar to that in the parent molecule (EAB). The selected optimized geometrical parameters for both stable conformers of EAB and their average for Me-EAB, Ph-EAB, and Bn-EAB at B3LYP/6-311++G(d,p) and MP2/6-311++G(d,p) levels are collected in Tables 1 and S1 (see supplementary material). The geometrical parameters of the mentioned molecules are also compared to the reported results for MAB [15]. EAB's chelated ring bond lengths (C2=C3, C2-N, C3-C4, and C4=O7) are similar to MAB's.

As previously reported, the N-Me and N-Ph groups in aminoketone molecules have more steric effect than the H atom [34]. Table 1 shows the calculated N···O distance (B3LYP/6-311++G(d,p)) in EAB, Me-EAB, Ph-EAB, Bn-EAB, and MAB, are 2.725, 2.721, 2.709, 2.722, and 2.728 Å, respectively. In addition, the calculated N-H and O···H distances in EAB, Me-EAB, Ph-EAB, Bn-EAB, and MAB are 1.014, 1.017, 1.022, 1.018, 1.014 Å̊, and 1.973, 1.912, 1.868, 1.909, 1.978 Å̊, respectively. The mentioned values indicate that the trend of the IHB strength of the mentioned molecules is:

$$\text{Ph-EAB} > \text{Bn-EAB} \sim \text{Me-EAB} > \text{EAB} \sim \text{MAB} \qquad (1)$$

Also, by comparing the structural parameters of EAB with the other substations, it can be concluded that the replacement of hydrogen atoms by Me, Ph, or Bn groups would reduce the C3-C2-N angle. At the same time, it increases the NHO, C2-C3-C4, and C3-C4-O8 bond angles.

The main effect of the ethoxy group ($–OC_2H_5$) or methoxy group ($–OCH_3$) on the C4 atom is to increase the N···O distance and decrease the N–H bond length, compared to the corresponding values of (Z)-4-aminopent-3-en-2-one (APO) [15]. The N···O distance and N–H bond length of APO at B3LYP/6-311++G(d,p) are 2.666 and 1.885 Å, respectively [15]. Soltani et al. [35] obtained an excellent correlation between the IHB strength and the N−H+H···O distances. The calculated N−H+H···O distances at B3LYP/6-311++G(d,p) in EAB, Me-EAB, Ph-EAB, Bn-EAB, and MAB are 2.988, 2.930, 2.891, 2.927, and 2.992 Å, respectively. These values also confirmed the trend of the IHB strength (1). The higher hydrogen bond strength in Ph-EAB is not related to the resonance of the phenyl with the chelated rings, as the dihedral angle between these two rings is 139.9º. It is due to the steric effect of the phenyl ring.

Table 2 shows some theoretical and experimental parameters related to the hydrogen bond strength (including the optimized geometrical parameters, AIM and NBO, and the results of different spectroscopic properties) for EAB, Me-EAB, Ph-EAB, Bn-EAB, and MAB [15, 36]. Some of these parameters, such as AIM, NBO, and spectroscopic results, are mentioned in the following sections, but since these parameters are related to the strength of the hydrogen bond, we have included them in this section.

In addition to geometric parameters such as the calculated N-H bond length, O···H, N···O, and N-H···O distances, and NHO bond angle in mentioned molecules, higher electron density (ρ_{BCP}) and minimum of Laplacian of the electron density ($\nabla^2\rho_{BCP}$) of the bond critical points (BCP) at O7···H10 corresponds to a stronger intramolecular hydrogen bond strength too. The E_{HB} values, in the gas phase, according to Espinosa et al. [37], are 8.27, 7.51, 7.41, 6.05, and 6.20 kcal/mol in Ph-EAB, Bn-EAB, Me-EAB, EAB, and MAB, respectively. Also, the LP(2)O7→σ*N-H10 interaction values confirm the trend (1) for IHB strength. In addition, based on spectroscopic results, the order of hydrogen bond strength agrees with the previous theoretical results (geometrical, NBO, and AIM results).

4.2. Second-order perturbation and pairwise steric exchange analyses

Table 3 shows some selected second-order perturbation ($E^{(2)}$) and pairwise steric exchange energies (ΔE (i, j)), related to IHB strength. The interactions such as LP(1)N9→ π*C2-C3, πC2-C3→ π*C4-O7, and LP(2)O7→ σ*C3-C4 show that the π-delocalization in the chelated rings of Me-EAB, Ph-EAB, and Bn-EAB is higher than in EAB. Furthermore, the values for the Ph-EAB is larger than those for Me-EAB and Bn-EAB so its IHB strength is the highest. Also, the LP(2)O7→σ* N9-H10 interaction and summation of interactions in this table, which are related to IHB strength, confirmed the trend (1).

Besides the LP(O7)↔σN9-H10 steric exchange interaction energies, ΔE (i,j), for EAB, Me-EAB, Bn-EAB, Ph-EAB and MAB are: 7.62, 9.92, 9.73, 11.89 and 7.59 kcal/mol, respectively. These values again support trend (1) for hydrogen bond strength. In addition, the steric effect of methyl, benzyl and phenyl moieties in that order increase the resonance in the chelate ring and the IHB strength. This agrees with the reported work on the 3-MeAPO (3-methyl-4-amino-3-penten-2-one) and its N-Me and N-Ph substitutions [34].

< Table 3 >

4.3. NMR spectroscopy

The ^{1}HNMR and ^{13}CNMR spectra of EAB and derivatives are shown in Fig. S3 (see supplementary materials). The measured chemical shifts (δ) and isotropic nuclear shielding (δ_{iso}) are listed in Table 4. The chemical changes agree with the previously reported results [38-40].

< Table 4 >

The experimental ^{1}H and ^{13}C chemical shifts ($\delta_{exp.}$) and the GIAO nuclear shielding ($\sigma_{calc.}$) calculated by DFT at the B3LYP/6-311++G(d,p) level is usually linear and described by the following equation: $\delta_{exp}=a(\sigma_{calc.})+b$. The equation for ^{1}H-NMR EAB is: 1.0165X+0.0328 (X is σ_{calc}) R^2=0.9943 and for ^{13}C-NMR including all four compounds is: 1.0429 X +1.605(X is σ_{calc}) R^2 = 0.9982 (see Fig. S4, see supplementary materials). The calculated and experimental δNH´s (in $CDCl_3$) of all molecules confirm the trend (1) in IHB strength. The broad NH resonances seen in the ^{1}H spectrum of EAB are due to the intermediate rotation of the NH_2 group because of the relatively weak intramolecular hydrogen bond.

4.4. UV–Vis spectra

In the β-ketoenamine, β-diketone, and β-ketoester compounds, the broad band in the region of about 300 nm can be due to chelated ring and IHB strength, too [34, 41]. The shifting of this band to higher wavelengths (red shifts) shows the increase in IHB strength. The UV spectra of EAB, Me-EAB, Ph-EAB, and Bn-EAB were recorded in ethanol (see Fig. S5, supplementary materials). Broad band at 274, 283, 300, and 277 nm were found for EAB, Me-EAB, Ph-EAB, and Bn-EAB, respectively. This band in the UV spectrum of MAB was reported at 272 nm [42]. The calculated UV wavelengths for EAB, Me-EAB, Ph-EAB, Bn-EAB, and MAB are 250, 264, 293, 265, and 250 nm, respectively, which are assigned to the HOMO→LUMO gap. These calculated and experimental values confirmed the trend (1) for IHB strength too. The calculated energy gaps between HOMO and LUMO, ΔE_{H-L}, in titled molecules with their orbital composition distribution were shown in Fig. S6 (see supplementary materials). The calculated ΔE_{H-L} in EAB, Me-EAB, Ph-EAB, and Bn-EAB are 5.34, 5.17, 4.62, and 5.11 eV, respectively.

4.5. Vibrational assignment

The IR spectra of EAB and its deuterated analog, D_3-EAB, in the CCl_4 solution are compared in Fig. 4a-b. In addition, Fig. 5 shows the Far-IR spectra of EAB and its deuterated analog in CCl_4. The deconvoluted IR spectrum of EAB in the CCl_4 solution and its IR spectrum in neat indicated is shown in Fig. S7 (see supplementary material). Also, the Raman spectrum of EAB in the liquid phase was given in Fig. 6. The computed scaled frequencies of vibrational harmonic bands and their approximate assignment, along with the experimental results of infrared frequencies for the stable aminoketone forms of EAB and its corresponding deuterated forms are presented in Tables 5 and 6, respectively. The assignment was compared to those reported for APO [43] and MAB [15] to support the assignments. The IR spectra of EAB in the liquid phase and MAB in the solid phase in the 3600–500 cm^{-1} region are compared (see Fig. S8).

The proper scaling factor, 0.9609 for upper 2000 cm^{-1} and 0.9859 for below 2000 cm^{-1} regions, are used for theoretical numbers [44]. Most frequencies of AK1 and AK2 conformers of EAB and D_3-EAB analog are near each other. However, Tables 5 and 6 indicate a few wavenumbers which occur in different places for two forms, which confirms the existence of both conformers in the sample.

The IR spectra of Me-EAB and Ph-EAB and their deuterated isotopomers, D_2Me-EAB and D_2Ph-EAB, in the CCl_4 solution are shown in Figs. S9-S10 (see supplementary material). Also, the IR spectrum of Bn-EAB in the CCl_4 solution is shown in Figs. S11 (see supplementary material). Fundamental band assignments for Ph-EAB and Bn-EAB are reported in Tables S2-S3 (see supplementary material). These tables show several bands in different regions confirming the presence of both conformers AK1 and AK2 in these compounds that agree with the reported work by Hansen *et al.* [19].

<Fig. 4>

<Fig. 5>

<Fig. 6>

<Table 5>

<Table 6>

The NH and CH stretching

In the aminoketone compounds, the symmetrical and asymmetrical NH stretching vibrations can be perturbed by intermolecular and intramolecular hydrogen bonds [45]. For example, in the CCl_4 solution, the symmetrical and asymmetrical stretching bands (ν_sNH and ν_aNH) of MAB and APO are reported at 3335, 3184, and 3447, 3375 cm^{-1}, respectively [15, 43]. This perturbation has been affected by the strength of the hydrogen bond.

the IR spectrum of EAB in CCl_4 solution shows two bands at 3449 and 3334 cm^{-1}. Upon deuteration of the NH_2 protons (hydrogen atoms with numbering of 10 and 12). These bands disappear and shift to 2587 and 2441 cm^{-1} (see Fig. 4 and Tables 5-6). This assigns the bands 3449 and 3334 cm^{-1} to the $\nu_a NH_2$ and $\nu_s NH_2$, respectively. These bands in a neat phase of EAB were observed at 3446 and 3335 cm^{-1}, respectively. This shows that EAB's intramolecular hydrogen bond strength is similar to MAB's. The IR band in the CCl_4 solution at 3512 cm^{-1} was assigned to NH_2 free, which was observed at 2625 cm^{-1} in the deuterated molecule. The corresponding Raman bands of $\nu_a NH_2$ and $\nu_s NH_2$ are observed at 3427 and 3320 cm^{-1}, respectively. The NH stretching of their N-Me, N-Ph, and N-Bn substitutions was observed at 3295, 3254, 3289 cm^{-1}, respectively [19]. The mentioned values agree with trend (1) for IHB strength.

The IR spectrum of EAB in the CCl_4 solution shows a weak band at 3230 cm^{-1}. We believe this band is an overtone of IR at 1616 cm^{-1}. This band was observed in 3-MeAPO at 3200 cm^{-1} [34].

The fragile intensity IR band of CCl_4 solution at 3088 cm^{-1}, which disappeared upon deuteration of Hα, is assigned to the olefinic CHα stretching mode and agrees with the theoretical calculations. The corresponding band in MAB/D_3-MAB [15] occurs at 3080/2297 cm^{-1}. This movement appeared at 2301 cm^{-1} in deuterated molecules.

The CH bond's stretching of the CH_3 groups generally appears in the 2900-3000 cm^{-1} region [46, 47]. The IR spectrum of EAB in the CCl_4 solution indicates six bands with relatively medium to weak intensity at 2984, 2955, 2935, 2902, 2872, and 2845 cm^{-1}, which are assigned to the CH stretching modes of the CH_3 and CH_2 groups. The corresponding Raman bands were observed at 2986, 2938, 2911, and 2877 cm^{-1}.

1700-1000 cm^{-1} region.

Besides the ρ (in-plane rocking) and δ (in-plane bending) modes of NH_2 and CH_3, other bands are expected to be observed in this region related to the vibrations of C-CH_3 and the chelated ring stretching, which arise from the C=C, C-C, C=O, and C-N stretching modes.

The IR spectrum of EAB in the CCl_4 solution shows three intense bands at 1670, 1616, and 1565 cm^{-1} (see Fig. S7). The corresponding Raman bands of EAB were observed at 1660, 1610, and 1555 cm^{-1} (see Fig. 6). According to the theoretical results, the band at 1670 cm^{-1} is assigned to ν_aO=C-C=C coupled to δNH_2 and ν_sN-C=C-C. We assign the IR band at 1616 cm^{-1} to the δNH_2 coupled to νsO=C-C=C, ν_sN-C=C-C. For APO and MAB, the corresponding bands in CCl_4 solution occurs at 1630, 1599 cm^{-1} and 1675, 1614 cm^{-1}, respectively [15, 43]. The mentioned values show that EAB's intramolecular hydrogen bond strength is almost equal to MAB and significantly lower than APO. In N-Me and N-Ph substitutions, the mentioned bands have shown a red shift and appeared at 1650 (1656) and 1615 (1620). These values in parenthesis are due to N-Ph substitution. These bands in N-Bn are 1660 and 1613 cm^{-1} too. The small difference between the mentioned values of N-Me, N-Ph, and N-Bn substitutions is attributed to different coupling and different of intramolecular hydrogen bond strength.

The band at 1565 cm^{-1} of EAB, is assigned to the NH_2 bending coupled with ν_sO=C-C=C. Upon deuteration, this band disappears, and the new band appears at about 1135 cm^{-1}, while the bands at 1670 and 1616 cm^{-1} shifted to 1663 and 1583 cm^{-1}, respectively.

The medium to weak intensity IR bands at 1480-1363 cm^{-1} region, that deuteration has not much effect on their wavenumbers, are assigned to δCH_3 and scissoring and wagging of CH_2, which were coupled to some other motions. According to theoretical results, the medium IR bands at 1305 cm^{-1} were assigned to ωCH_2 for AK2. This band in N-Me substitution also appeared at 1301 cm^{-1} for AK2 [19]. The existence of this band approved the presence of AK1 and AK2 in the sample.

The relatively sharp IR band at 1166 cm^{-1} and its shoulder at 1174 cm^{-1} are assigned to the δCHα coupled to ν_aC-O-C, ρNH_2 for both stable conformers. According to calculated results and compared to MAB [15], two weak intensity IR bands at 1117 and 1097 cm^{-1} are assigned to the rocking of NH_2 and ρNH_2, coupled with other movements for AK1 and AK2. In addition, according to calculated results, three IR bands at 1095,

1088, and 1065 cm^{-1} in the deuterated form of EAB are also due to the existence of both stable conformers. At low temperatures, two rotamers were also observed in the comparable compound 2-aminobenzoate [48].

Also, the presence of the bands at 1095, 975, 960, and 982, 977, 935 cm^{-1} in the IR spectra confirm the existence of both conformers of AK1 and AK2 in Ph-EAB, and Bn-EAB, respectively (see Tables S2-S3, see supplementary materials).

Below 1000 cm^{-1} region.

Two IR bands at about 977 and 960 cm^{-1} of EAB and D_3EAB, assigned to ν_sC3-C4-O8, $\rho C1H_3$ of AK1 and AK2 too. The medium IR band at 786 cm^{-1} was assigned to out-of-plane bending of CHα, γCHα. In deuterated form, it appeared at 560 cm^{-1}. In MAB γCH/γCD were reported at 786/560 cm^{-1} [15]. According to calculated results and compared to MAB [15], the broad IR band at 675 cm^{-1} is assigned to γNH_2, that in deuterated form appeared at 450 cm^{-1}. According to theoretical results, the IR bands at 444 and 425 cm^{-1} are assigned to in-plane bending of the chelated ring Δ, which was coupled with other motions. The IR bands at 330 and 275 cm^{-1} are assigned to N…O stretching and γNH, respectively. The different values of N…O stretching in MAB and EAB are due to different coupling.

5. Conclusion

Ethyl 3-amino-2-butenoates were synthesized and characterized by FT-IR, UV, ^{1}H, and ^{13}C NMR. The theoretical and experimental results showed that the keto-enamine tautomers are the most stable. Among all of the keto-enamine tautomers with NH…O hydrogen bonds, two conformers (AK1 and AK2) are present. Also, the existence of these conformers of EAB, Ph-EAB, and Bn-EAB are confirmed by vibrational spectroscopy. An excellent agreement was achieved between experimental results (δNH, νNH, γNH, UV) and theoretical results (geometrical parameters, AIM, NBO, vibrational) with the E_{HB}. All theoretical and experimental results show that the following trend in IHB strength is obtained:

Ph-EAB > Bn-EAB ~ Me-EAB > EAB ~ MAB

Acknowledgements

The authors are grateful to the Ferdowsi University of Mashhad for financial support of this work (Grant No. 45066).

The authors wish to thank Eva Marie Karlsen (Roskilde University) for scanning of IR and UV spectra of EAB, Me-EAB, Bn-EAB, and Ph-EAB molecules.

Supplementary Information

Additional supporting information can be found in Tables S1-3 and Figures S1-11 in supplementary materials

Author contributions

Mr. Mahmoud Bazrafshan: Methodology, Formal analysis and investigation, writing original draft

Dr. Mohammad Vakili *: Conceptualization, Supervision, Writing-review and editing

Prof. Sayyed Faramarz Tayyari: Supervision, Writing-review and editing

Dr. Fadhil S. Kamounah: preparation, Writing-review and editing

Prof. Poul Erik Hansen, Writing-review and editing

Dr. Ali Shiri, Writing-review and editing

Funding

The authors did not receive support from any organization for the submitted work.

Declarations

Consent to participate

All authors agreed to participate in this research.

Competing interests

The authors declare that they have no conflict of interest.

References

[1] J. Greenhill, Enaminones, Chem. Soc. Rev. 6 (1977) 277-294. https://doi.org/10.1039/CS9770600277.

[2] I. Chaaban, J.V. Greenhill, P. Akhtar, Enaminones in the mannich reaction. Part 2. Further investigations of internal mannich reactions, J. Chem. Soc., Perkin trans. (1979) 1593-1596. https://doi.org/10.1039/P19790001593.

[3] J.P. Michael, C.B. De Koning, D. Gravestock, G.D. Hosken, A.S. Howard, C.M. Jungmann, R.W. Krause, A.S. Parsons, S.C. Pelly, T.V. Stanbury, Enaminones: Versatile intermediates for natural product synthesis, Pure Appl. Chem. 71 (1999) 979-988. https://doi.org/10.1351/pac199971060979.

[4] A.C. Spivey, R. Srikaran, C.M. Diaper, D.J. Turner, Traceless solid phase synthesis of 2-substituted pyrimidines using an 'off-the-shelf'chlorogermane-functionalised resin, Org. Biomol. Chem. 1 (2003) 1638-1640. https://doi.org/10.1039/B303064D.

[5] D.L. Boger, T. Ishizaki, R.J. Wysocki Jr, S.A. Munk, P.A. Kitos, O. Suntornwat, Total synthesis and evaluation of (.+-.)-n-(tert-butoxycarbonyl)-cbi,(.+-.)-cbi-cdpi1, and (.+-.)-cbi-cdpi2: Cc-1065 functional agents incorporating the equivalent 1, 2, 9, 9a-tetrahydrocyclopropa [1, 2-c] benz [1, 2-e] indol-4-one (cbi) left-hand subunit, J. Am. Chem. Soc. 111 (1989) 6461-6463. https://doi.org/10.1021/ja00198a089.

[6] J.E. Foster, J.M. Nicholson, R. Butcher, J.P. Stables, I.O. Edafiogho, A.M. Goodwin, M.C. Henson, C.A. Smith, K. Scott, Synthesis, characterization and anticonvulsant activity of enaminones. Part 6: Synthesis of substituted vinylic benzamides as potential anticonvulsants, Bioorg. Med. Chem. 7 (1999) 2415-2425. https://doi.org/10.1016/S0968-0896(99)00185-6.

[7] E.-S.A. Badawey, I.M. El-Ashmawey, Nonsteroidal antiinflammatory agents-part 1: Antiinflammatory, analgesic and antipyretic activity of some new 1-(pyrimidin-2-yl)-3-pyrazolin-5-ones and 2-(pyrimidin-2-yl)-1, 2, 4, 5, 6, 7-hexahydro-3h-indazol-3-ones, Eur. J. Med. Chem. 33 (1998) 349-361. https://doi.org/10.1016/S0223-5234(98)80002-0.

[8] J.P. Michael, C.B. de Koning, G.D. Hosken, T.V. Stanbury, Reformatsky reactions with n-arylpyrrolidine-2-thiones: Synthesis of tricyclic analogues of quinolone antibacterial agents, Tetrahedron 57 (2001) 9635-9648. https://doi.org/10.1016/S0040-4020(01)00964-4.

[9] J.P. Michael, D. Gravestock, Enaminones as intermediates in the synthesis of indolizidine alkaloids, Pure Appl. Chem. 69 (1997) 583-588. https://doi.org/10.1351/pac199769030583.

[10] L.J. Figueiredo, C. Kascheres, Quinone diazides and enaminones as a source of new azo compounds with potential nonlinear optical properties, J. Org. Chem. 62 (1997) 1164-1167. https://doi.org/10.1021/jo9604907.

[11] L.F. Tietze, E. Voß, Synthesis of 3-amino sugars of the daunosamine type through hetero-diels-alder reaction of enaminones, Tetrahedron Lett. 27 (1986) 6181-6184. https://doi.org/10.1016/S0040-4039(00)85427-1.

[12] R. Aumann, B. Jasper, R. Froehlich, Organic syntheses via transition metal complexes. 75. Phosphinonaphthalenes and phosphinoindenes by cyclization of alkynyl carbene complexes (m= cr, w), Organometallics 14 (1995) 231-237. https://doi.org/10.1021/om00001a035.

[13] R. SanMartín, E.M. de Marigorta, E. Domínguez, A convenient alternative route to β-aminoketones, Tetrahedron 50 (1994) 2255-2264. https://doi.org/10.1016/S0040-4020(01)85083-3.

[14] M.A. Harrad, R. Outtouch, M.A. Ali, L. El Firdoussi, A. Karim, A. Roucoux, Ca (cf3coo) 2: An efficient lewis acid catalyst for chemo-and regio-selective enamination of β-dicarbonyl compounds, Catal. Commun. 11 (2010) 442-446. https://doi.org/10.1016/j.catcom.2009.11.019.

[15] A.R. Berenji, S.F. Tayyari, M. Rahimizadeh, H. Eshghi, M. Vakili, A. Shiri, Structure and vibrational analysis of methyl 3-amino-2-butenoate, Spectrochim. Acta A 102 (2013) 350-357. https://doi.org/10.1016/j.saa.2012.10.042.

[16] R. Singh, H. Bhatia, P. Prakash, E. Debroye, S. Dey, W. Dehaen, Tandem nenitzescu reaction/nucleophilic aromatic substitution to form novel pyrido fused indole frameworks, Eur. J. Org. Chem. 2021 (2021) 4865-4875. https://doi.org/10.1002/ejoc.202100827.

[17] R.F. Bader, Atoms in molecules, Wiley Online Library, 1990.

[18] S.F. Tayyari, M. Ghafari, M. Jamialahmadi, B. Chahkandi, B.O. Patrick, Y.A. Wang, Vibrational assignment and crystal structure of 3-amino-1-phenyl-2-buten-1-one, J. Mol. Struct. 1045 (2013) 20-28. https://doi.org/10.1016/j.molstruc.2013.04.029.

[19] P.E. Hansen, M. Vakili, F.S. Kamounah, J. Spanget-Larsen, Nh stretching frequencies of intramolecularly hydrogen-bonded systems: An experimental and theoretical study, Molecules 26 (2021) 7651-7675. https://doi.org/10.3390/molecules26247651.

[20] C. Lee, W. Yang, R.G. Parr, Development of the colle-salvetti correlation-energy formula into a functional of the electron density, Phys. Rev. B 37 (1988) 785-789. https://doi.org/10.1103/PhysRevB.37.785.

[21] B. Miehlich, A. Savin, H. Stoll, H. Preuss, Results obtained with the correlation energy density functionals of becke and lee, yang and parr, Chem. Phys. Lett. 157 (1989) 200-206. https://doi.org/10.1016/0009-2614(89)87234-3.

[22] G.W.T. M. J. Frisch, H. B. Schlegel, G. E. Scuseria, M. A. Robb, J. R. Cheeseman, G. , V.B. Scalmani, B. Mennucci, G. A. Petersson, H. Nakatsuji, M. Caricato, X. Li, H. P. , A.F.I. Hratchian, J. Bloino, G. Zheng, J. L. Sonnenberg, M. Hada, M. Ehara, K. Toyota, , J.H. R. Fukuda, M. Ishida, T. Nakajima, Y. Honda, O. Kitao, H. Nakai, T. Vreven, J. A. , J.E.P. Montgomery Jr., F. Ogliaro, M. Bearpark, J. J. Heyd, E. Brothers, K. N. Kudin, V. N. , R.K. Staroverov, J. Normand, K. Raghavachari, A. Rendell, J. C. Burant, S. S. Iyengar, J. , M.C. Tomasi, N. Rega, J. M. Millam, M. Klene, J. E. Knox, J. B. Cross, V. Bakken, C. , J.J. Adamo, R. Gomperts, R. E. Stratmann, O. Yazyev, A. J. Austin, R. Cammi, C. , J.W.O. Pomelli, R. L. Martin, K. Morokuma, V. G. Zakrzewski, G. A. Voth, P. Salvador, , S.D. J. J. Dannenberg, A. D. Daniels, Ö. Farkas, J. B. Foresman, J. V. Ortiz, J. Cioslowski, , D.J. Fox, Gaussian 09, revision d. 01, Gaussian, Inc., Wallingford CT, 2009.

[23] R. Dennington, T. Keith, J. Millam, Gaussview, version 5, (2009).

[24] M.J. Frisch, M. Head-Gordon, J.A. Pople, A direct mp2 gradient method, Chem. Phys. Lett. 166 (1990) 275-280. https://doi.org/10.1016/0009-2614(90)80029-D.

[25] C. Møller, M.S. Plesset, Note on an approximation treatment for many-electron systems, Phys. Rev. 46 (1934) 618–622. https://doi.org/10.1103/PhysRev.46.618.

[26] F. Biegler-König, J. Schönbohm, Update of the AIM2000 program for atoms in molecules. J. comp. chem., 23(15), (2002) 1489-1494. https://doi.org/10.1002/jcc.10085.

[27] A.E. Reed, L.A. Curtiss, F. Weinhold, Intermolecular interactions from a natural bond orbital, donor-acceptor viewpoint, Chem. Rev. 88 (1988) 899-926. https://doi.org/10.1021/cr00088a005.

[28] V.F. Weisskopf, Of atoms, mountains, and stars: a study in qualitative physics, Science 187 (1975) 605-612.

[29] E. D. Glendening, J. K. Badenhoop, A. E. Reed, J. E. Carpenter, J. A. Bohmann, C. M. Morales, F. Weinhold, Theoretical Chemistry Institute, University of Wisconsin, Madison, WI, NBO 5.0., 2001.

[30] S. Miertuš, E. Scrocco, J. Tomasi, Electrostatic interaction of a solute with a continuum. A direct utilizaion of ab initio molecular potentials for the prevision of solvent effects, Chem. Phys. Lett. 55 (1981) 117-129. https://doi.org/10.1016/0301-0104(81)85090-2.

[31] K. Wolinski, J.F. Hinton, P. Pulay, Efficient implementation of the gauge-independent atomic orbital method for nmr chemical shift calculations, J. Am. Chem. Soc. 112 (1990) 8251-8260. https://doi.org/10.1021/ja00179a005.

[32] K. Woliński, A.J. Sadlej, Self-consistent perturbation theory: Open-shell states in perturbation-dependent non-orthogonal basis sets† this work was partly supported by the institute of low temperatures and structure research of the polish academy of sciences under contract no. Mr-i. 9.4. 3/2, Mole. Phys. 41 (1980) 1419-1430. https://doi.org/10.1080/00268978000103631.

[33] S.F. Tayyari, B. Chahkandi, S. Mehrani, R.W. McClurg, C.A. Keyes, R.E. Sammelson, Conformational analysis, tautomerization, ir, raman, and nmr studies of ethyl benzoylacetate, J. Mol. Struct. 1015 (2012) 74-85. https://doi.org/10.1016/j.molstruc.2010.12.034.

[34] S. Seyedkatouli, M. Vakili, S.F. Tayyari, P.E. Hansen, F.S. Kamounah, Molecular structure and intramolecular hydrogen bond strength of 3-methyl-4-amino-3-penten-2-one and its nme and n-ph substitutions by experimental and theoretical methods, J. Mol. Struct. 1184 (2019) 233-245. https://doi.org/10.1016/j.molstruc.2019.02.007.

[35] S. Soltani-Ghoshkhaneh, M. Vakili, A.R. Berenji, V. Darugar, S.F. Tayyari, Conformations, molecular structure, and N–H⋯ O hydrogen bond strength in 4-alkylamino-3-penten-2-ones, J. Mol. Struct. 1203 (2020) 127440. https://doi.org/10.1016/j.molstruc.2019.127440.

[36] SDBSWeb:http://riodb01.ibase.aist.go.jp/sdbs/, 2012.

[37] E. Espinosa, E. Molins, C. Lecomte, Hydrogen bond strengths revealed by topological analyses of experimentally observed electron densities, Chem. Phys. Lett. 285 (1998) 170-173. https://doi.org/10.1016/S0009-2614(98)00036-0.

[38] L. Rout, A. Kumar, R.S. Dhaka, P. Dash, Bimetallic ag–cu alloy nanoparticles as a highly active catalyst for the enamination of 1, 3-dicarbonyl compounds, RSC advances 6 (2016) 49923-49940. https://doi.org/10.1039/C6RA04569C.

[39] S. Hirai, Y. Horikawa, H. Asahara, N. Nishiwaki, Tailor-made synthesis of fully alkylated/arylated nicotinates by fecl 3-mediated condensation of enamino esters with enones, Chem. Comm. 53 (2017) 2390-2393. https://doi.org/10.1039/C7CC00051K.

[40] D.S. Reddy, T.V. Rajale, K. Shivakumar, J. Iqbal, A mild and efficient method for the synthesis of vinylogous carbamates from alkyl azides, Tetrahedron Lett. 46 (2005) 979-982. https://doi.org/10.1016/j.tetlet.2004.12.047.

[41] V. Lazić, M. Jurković, T. Jednačak, T. Hrenar, J.P. Vuković, P. Novak, Intra-and intermolecular hydrogen bonding in acetylacetone and benzoylacetone derived enaminone derivatives, J. Mol. Struct. 1079 (2015) 243-249. https://doi.org/10.1016/j.molstruc.2014.09.048.

[42] https://spectrabase.com/spectrum/2U2eYcw9GRj.

[43] S.F. Tayyari, H. Raissi, F. Tayyari, Vibrational assignment of 4-amino-3-penten-2-one, Spectrochim. Acta A 58 (2002) 1681-1695. https://doi.org/10.1016/S1386-1425(01)00620-5.

[44] S.F. Tayyari, T. Bakhshi, S.J. Mahdizadeh, S. Mehrani, R.E. Sammelson, Structure and vibrational assignment of magnesium acetylacetonate: A density functional theoretical study, J. Mol. Struct. 938 (2009) 76-81. https://doi.org/10.1016/j.molstruc.2009.09.006.

[45] J. Gardner, A. Katritzky, 875. N-oxides and related compounds. Part v. The tautomerism of 2-and 4-amino-and-hydroxy-pyridine 1-oxide, J. Chem. Soc. B DOI (1957) 4375-4385. https://doi.org/10.1039/JR9570004375.

[46] M.M. Borah, T.G. Devi, Vibrational studies of thyroxine hormone: Comparative study with quantum chemical calculations, J. Mol. Struct. 1148 (2017) 293-313. https://doi.org/10.1016/j.molstruc.2017.07.063.

[47] N. Colthup, Introduction to infrared and raman spectroscopy, Elsevier, 2012.

[48] J. Laane, M. Dakkouri, B. van der Veken, H. Oberhammer, Structures and conformations of non-rigid molecules, Springer Science & Business Media, 2012.

Table 1. Some selected parameters of EAB, Me-EAB, Ph-EAB, Bn-EAB, and MAB calculated at B3LYP and MP2 levels with 6-311++G(d,p) basis set.

	EAB				Me-EAB		Ph-EAB		Bn-EAB		MAB[a]	
	B3LYP			MP2	B3LYP	MP2	B3LYP	MP2	B3LYP	MP2	B3LYP	MP2
	AK1	AK2	Avg.	Avg.	Avg.	Avg.	Avg.	Avg.	Avg.	Avg.		
Bond length (Å)												
C1-C2	1.505	1.510	1.508	1.504	1.505	1.505	1.506	1.506	1.505	1.504	1.505	1.504
C2=C3	1.369	1.371	1.370	1.367	1.376	1.375	1.374	1.374	1.375	1.372	1.369	1.367
C2-N	1.354	1.352	1.353	1.366	1.353	1.361	1.364	1.365	1.357	1.370	1.355	1.366
C3-C4	1.446	1.444	1.445	1.453	1.439	1.448	1.443	1.448	1.440	1.451	1.444	1.452
C4=O7	1.229	1.230	1.230	1.229	1.232	1.232	1.231	1.233	1.232	1.232	1.228	1.228

C4-O8	1.359	1.361	1.360	1.358	1.361	1.360	1.357	1.358	1.360	1.357	1.360	1.358
O8-C5	1.443	1.444	1.444	1.440	1.443	1.439	1.444	1.441	1.443	1.441	1.434	1.433
C5-C6	1.516	1.521	1.518	1.517	1.519	1.517	1.519	1.517	1.519	1.517	….	….
N-H10	1.014	1.015	1.015	1.015	1.017	1.018	1.022	1.022	1.018	1.019	1.014	1.015
N-H12(or C)	1.005	1.004	1.005	1.008	1.450	1.452	1.411	1.413	1.451	1.456	1.005	1.008
N···O7	2.722	2.717	2.720	2.741	2.720	2.730	2.710	2.697	2.722	2.737	2.728	2.742
H10··· O7	1.971	1.962	1.967	1.985	1.912	1.917	1.869	1.878	1.909	1.908	1.978	1.987
Bond angles (°)												
C1C2C3	121.1	120.5	120.8	121.2	120.2	120.2	119.3	120.1	120.0	120.7	12 1.1	121.2
C1C2N	115.7	116.5	116.1	115.2	117.4	116.9	119.7	118.3	117.8	116.7	115.8	115.2
C2C3C4	122.3	122.4	122.4	122.2	122.7	122.4	123.4	122.4	122.9	122.5	122.4	122.2
C3C4O7	126.1	125.9	126.0	126.2	126.0	126.2	125.9	126.0	126.1	126.3	126.3	126.4
C3C2N	123.1	123.2	123.2	123.5	122.5	122.8	120.9	121.5	122.2	122.6	….	….
C3C4O8	112.3	112.1	112.2	111.5	112.3	111.7	112.2	111.9	112.3	111.6	112.2	111.6
C4O8C5	116.5	117.3	116.9	115.2	116.9	115.2	117.4	115.3	117.0	115.3	116.0	114.4
HNH (or C)	120.8	121.0	120.9	118.0	119.6	118.0	116.8	119.2	119.3	116.1	120.5	117.9
C2C3H11	119.5	119.4	119.5	119.6	119.4	119.5	119.1	119.4	119.3	119.6	119.6	119.6
NHO	128.7	128.9	128.8	129.1	134.1	134.7	137.3	134.9	134.6	136.3	128.6	129.0

[a] Data source: Ref. [15].

Table 2. Comparing several properties related to the hydrogen bond strength for EAB, Me-EAB, Ph-EAB, Bn-EAB, and MAB calculated at B3LYP/6-311++G(d,p) level of theory.[a]

	EAB	Me-EAB	Ph-EAB	Bn-EAB	MAB[e]
Geometrical result [b]					
RN–H	1.014	1.017	1.022	1.018	1.014
RN-H···O	2.988	2.930	2.891	2.927	2.992
RH···O	1.973	1.912	1.868	1.909	1.978
RN···O	2.725	2.721	2.709	2.722	2.728
θNHO	128.7	134.1	137.3	134.6	128.6
AIM and NBO results [c]					
ρ_{BCP}	0.0258	0.0299	0.0331	0.0303	0.0262[f]
$\nabla^2\rho_{BCP}$	-0.0240	-0.0272	-0.0292	-0.0275	-0.0245[f]
H-bond energy	6.05	7.41	8.27	7.51	6.20[f]
LP(2)O7 → σ*N-H10	5.21	6.77	8.65	7.18	5.11[f]
Spectroscopic results [d]					
δNH	8.12 (7.90)	8.62 (8.46)	10.88 (10.39)	9.53 (8.95)	8.44[f] (7.83[g])
νNH	3703 (3334)	3469 (3294)	3388 (3255)	3463 (3290)	3506(3335)
UV (π→π*)	250 (274)	262 (283)	293 (300)	265 (277)	250[f] (272)

[a] All theoretical values are given the averages AK1-2 for EAB, Me-EAB, Ph-EAB, and Bn-EAB.
[b] R is bond length in Å, θ is bond angle in degree.
[c] The units of AIM results are: ρ_{BCP} (e au^{-3}), $\nabla^2\rho_{BCP}$ (e au^{-5}), and H-bond energy E_{HB}; hydrogen bond energies (E_{HB}/kcal mol^{-1}=1/2V) [39] (kcalmol^{-1}).
[d] ν is stretching modes frequencies, in cm^{-1}. δ, proton chemical shift in ppm, and UV bands in nm. (Experimental values are given in parenthesis).
[e] Data from Ref. [15].
[f] Calculated this work.
[g] Data from Ref. [44].

Table 3. Selected second order perturbation energies, $E^{(2)}$, in kcal/mol, of EAB, Me-EAB, Ph-EAB, Bn-EAB, and MAB.

Donor	Type	Acceptor	Type	EAB	Me-EAB	Ph-EAB	Bn-EAB	MAB
N	LP(1)	C2-C3	π*	45.64	84.38	85.94	57.89	56.40
O7	LP(2)	N-H10	σ*	4.91	6.77	8.73	7.25	5.11
O7	LP(2)	C3-C4	σ*	13.95	16.21	16.71	12.76	13.52
O7	LP(1)	C4	RY*(1)	14.84	11.59	18.79	14.39	15.25
O7	CR(1)	C4	RY*(1)	6.19	6.56	6.53	6.17	6.29
C2-C3	π	O7-C4	π*	27.63	48.76	50.67	4.72	29.02

Table 4. Experimental, calculated, and estimated ^{13}C and ^{1}H chemical shifts (δ) and isotropic nuclear shildings (σ_{iso}) for stable forms of EAB, Me-EAB, Ph-EAB, Bn-EAB.[a]

	EAB		Me-EAB		Ph-EAB		Bn-EAB	
Carbon-13	$\delta_{exp}(\delta_{cal})$	σ_{iso}	$\delta_{exp}(\delta_{cal})$	σ_{iso}	$\delta_{exp}(\delta_{cal})$	σ_{iso}	$\delta_{exp}(\delta_{cal})$	σ_{iso}
C1	22.42 (22.41)	160.11	19.28 (21.86)	162.66	20.36 (23.88)	160.64	19.44 (21.64)	30.98
C2	159.77 (170.56)	13.96	162.91 (172.66)	11.86	158.96 (169.02)	15.50	161.89 (170.32)	179.55
C3	84.24 (92.23)	92.29	81.99 (87.85)	96.67	86.13 (91.37)	93.15	83.25 (86.06)	57.32
C4	170.36 (178.82)	5.70	170.79 (178.91)	5.61	170.44 (179.38)	5.14	170.66 (175.65)	99.94
C5	58.61 (64.13)	120.39	58.38 (63.72)	120.80	58.80 (64.33)	120.19	58.46 (63.87)	60.85
C6	14.68 (16.78)	167.74	14.76 (16.98)	167.54	14.66 (16.91)	167.61	14.71 (16.73)	25.67
C12	…	…	29.67 (31.42)	153.10	139.42 (149.20)	35.32	46.85 (50.63)	38.06
C13	…	…	…	…	124.95 (133.17[d])	51.35[d]	138.82 (150.12)	190.13
C14	…	…	…	…	129.10 (137.11[d])	47.42[d]	126.77 (132.28[e])	179.36[e]
C15	…	…	…	…	124.45 (135.11)	49.41	126.77 (132.28[e])	179.36[e]
C16	…	…	…	…	129.10 (137.11[d])	47.42[d]	138.82 (135.74[e])	186.25[e]
C17	…	…	…	…	124.95 (133.17[d])	51.35[d]	138.82 (135.74[e])	186.25[e]
C18	…	…	…	…	…	…	127.40 (133.39)	183.89
Proton								
H1(CH_3-C-N)[b]	1.88 (1.98)	30.00	1.90 (1.98)	29.99	1.99 (1.99)	29.98	1.90 (1.83)	6.77
H3(C-CH-C)[b]	4.50 (4.95)	27.02	4.45 (4.78)	27.19	4.69 (5.04)	26.93	4.53 (4.79)	7.73
H5(O-CH_2-C)[b]	4.08 (4.13)	27.84	4.07 (4.11)	27.86	4.15 (4.20)	27.77	4.09 (4.18)	5.75
H6(CH_3-C-O)[b]	1.23 (1.30)	30.67	1.23 (1.24)	30.72	1.28 (1.33)	30.42	1.25 (1.28)	8.21
H10	7.90 (8.14)	23.83	8.46 (8.62)	23.35	10.39 (10.88)	21.09	8.95 (9.53)	16.46
H12	4.4–4.9 (4.16)	27.81	2.89 (2.93)	29.04	…	…	4.42 (4.55)	6.35
O-H[c]	…	…	…	…	7.08 (7.52)	24.46	7.26 (7.55)	8.60
m-H[c]	…	…	…	…	7.31 (7.75)	24.23	7.33 (7.63)	5.47
p-H[c]	…	…	…	…	7.14 (7.56)	24.41	7.26 (7.53)	4.59

[a] δ_{exp}, experimental chemical shifts in $CDCl_3$,δ_{cal}, calculated chemical shifts by $\delta = \sigma_0 - \sigma$ equation. All chemical shifts in Chloroform are relative to TMS, which its ^{13}C and proton magnetic shielding are 184.52 and 31.97 ppm, respectively. δ_{est}, estimated chemical shifts are obtained by using of the δ_{exp} vs. calculated nuclear shielding plot of EAB.

[b] The numbering of hydrogen atoms on methyl groups are as same as the corresponding carbon atoms.

[c] The ortho, meta, and para hydrogen atoms of Ph ring.

[d] Averaged values for 13, 17 and 14, 15 atoms of Ph-EAB.

[e] Averaged values for 14, 15 and 16, 17 atoms of Bn-EAB.

Table 5. Calculated energy values of EAB, Me-EAB, Ph-EAB, Bn-EAB, and MAB at B3LYP/6-311++G(d,p) level of theory.

	EAB	Me-EAB	Ph-EAB	Bn-EAB	MAB
E_{HOMO} (eV)	-6.300	-5.966	-5.989	-5.834	-6.074
E_{HOMO-1} (eV)	-7.762	-7.662	-7.289	-7.034	-7.424
E_{LUMO} (eV)	-0.944	-0.830	-1.227	-0.727	-0.730
E_{LUMO+1} (eV)	-0.250	-0.247	-0.751	-0.672	-0.432
$E_{HOMO–LUMO}$ gap (eV)	-5.356	-5.136	-4.762	-5.107	-5.344
chemical potential (μ)	3.622	3.398	3.608	3.281	3.402
Global hardness (η)	2.678	2.568	2.381	2.554	2.672
Global softness (S)	0.373	0.389	0.420	0.392	0.374
Elecronegativity (χ)	-3.622	-3.398	-3.608	-3.281	-3.402
Electrophilisity indices (ω)	2.449	2.248	2.734	2.107	2.166

Table 6. Experimental (FT-IR wavenumbers (in cm^{-1})) and theoretical (scaled wavenumbers (in cm^{-1})) of EAB at B3LYP/6-311++G(d,p) level of theory. [a]

No.	Theoretical						Experimental			Assignment
	AK1			AK2						
	Freq.	I_{IR}	A_R	Freq.	I_{IR}	A_R	IR(CCl_4)	IR(neat)	R(neat)	
							3512(18)			νNH_2free
1	3703	86	83	3703	86	82	3449(6,br)	3446(25)	3427(4)	$\nu_a NH_2$
2	3504	70	109	3504	70	109	3334(14)	3335(25)	3320(10)	$\nu_s NH_2$
							3230(w,br)	3233(4,br)		2*1616
3	3221	21	61	3222	21	62	3088(vw)	3084(vw)		νCHα
4	3134	114	47	3134	114	48	2984(14)	2982(19)	2986(14)	$\nu_a C1H_3$
5	3110	42	22	3125	29	8	2955(3)	2955(3)		$\nu_a CH_2$, $\nu_a C6H_3$
6	3099	31	94	3104	12	85	2935(4)	2938(4)	2938(22)	$\nu_a CH_2$, $\nu_a C6H_3$
7				3093	30	107	2935	2938	2938	$\nu_a C6H_3$, $\nu_a CH_2$
	3077	6	88				2902(4)	2902(6)	2911(11,sh)	$\nu_a C6H_3$, $\nu_a CH_2$
8	3073	12	108	3074	13	107	2902	2902	2911	$\nu_a C1H_3$
				3065	33	151	2902	2902	2911	$\nu_s CH_2$
9	3044	20	136				2872(2)	2873(2)	2877(sh)	$\nu_s CH_2$
10	3033	23	188	3031	23	199	2872	2873	2877	$\nu_s C6H_3$
11	3025	28	274	3025	29	273	2845(vw)	2845(1)		$\nu_s C1H_3$
12	1700	239	10	1700	219	10	1670(72)	1665(67)	1660(9)	ν_aO=C-C=C, δNH_2, ν_aN-C=C-C
							1632(36,sh)			Combination

13	1659	431	52	1658	440	54	1616(53)	1623(81)	1610(10)	δNH_2, $\nu_s O{=}C{-}C{=}C$, $\nu_s N{-}C{=}C{-}C$
14	1592	247	97	1591	245	96	1565(49)	1566(38)	1555(99)	δNH_2, $\nu_s O{=}C{-}C{=}C$
15	1521	4	3	1506	12	3	1480(4,sh)	1482(sh)		$SciCH_2$, $\delta_a C6H_3$
16	1498	4	11				1466(3,sh)	1465(sh)	1453(4)	$\delta_a C6H_3$, $SciCH_2$
				1493	32	30	1466	1465	1453	$sciCH_2$, $\delta_a C6H_3$, $\delta_a C1H_3$
17	1489	48	19				1445(11)	1447(8)	1440(4)	$\delta_a C1H_3$, δNH_2
				1488	6	15	1445	1447	1440	$\delta_a C6H_3$, $\delta_a C1H_3$, $SciCH_2$
18	1486	7	10				1445	1447	1440	$\delta_a C6H_3$
				1486	28	7	1445	1447	1440	$\delta_a C6H_3$, $\delta_a C1H_3$, $SciCH_2$
19	1483	10	8	1482	9	8	1425(4,sh)	1422(sh)		$\delta_a C1H_3$
20	1446	4	3	1445	2	6	1425	1422		$\nu_a CH_3{-}C{-}N$, $\delta_s C1H_3$, $\delta CH\alpha$, ωCH_2
21	1423	2	2	1418	10	2	1390(4,sh)	1389(sh)		$\delta_s C6H_3$, ωCH_2, $\delta_s C1H_3$
22	1411	10	10	1408	7	7	1377(10)	1377(12)	1380(6)	$\delta_s C1H_3$, $\delta_s C6H_3$, $\delta CH\alpha$
23	1393	3	4	1396	9	7	1363(10)	1360(17)	1355(7)	ωCH_2, $\delta_s C6H_3$
24				1334	35	7	1305(33)			ωCH_2, $\delta_s C6H_3$
25	1314	433	12	1314	347	10	1272(28)	1280(79)	1269(20)	$\nu_a C3{-}C4{-}O8$, ρNH_2, $\delta CH\alpha$, $\nu C2{-}C1$, ωCH_2
	1294	1	10						1235(12)	τCH_2, $\delta_s C6H_3$
26				1195	353	5	1174 (sh)	1173 (sh)		$\delta CH\alpha$, $\nu_a C{-}O{-}C$, ρNH_2
	1186	488	5				1166(100)	1165(100)		$\delta CH\alpha$, $\nu_a C{-}O{-}C$, ρNH_2
27	1176	3	11	1181	94	2	1166	1165		ρCH_2, $\rho C6H_3$
28	1135	4	16							$\pi C6H_3$, $\delta O8{-}C5{-}C6$
				1131	81	14	1117(11)	1114(8)	1110(10)	ρNH_2, $\rho C1H_3$, $\nu C5{-}O8$

2929	1132	628					1117		1110	ρNH_2, $\nu_a C{=}C\text{-}C\text{-}O$
				1113	17	2	1097(8)	1095(17)	1090(3)	ρNH_2, $\nu C5\text{-}C6$, $\rho C6H_3$
3061	1061	313	1	1061	2	1	1047(24)			$\pi C1H_3$
3160	1053	017		1053	0	9	1047	1046	1040(5)	$\nu_a C3\text{-}C4\text{-}O8\text{-}C5$, ρNH_2
3230	1026	272		1026	2	2	1015(6)	1014(11)		$\rho C1H_3$,$\nu_a O8\text{-}C5\text{-}C6$
3393	978(3)	977(8)							983(12)	$\nu_s C3\text{-}C4\text{-}O8$, $\nu C5\text{-}C6$, $\rho C1H_3$
				973	15	5	960(5)	960(9)	952(10)	$\nu_s C3\text{-}C4\text{-}O8$, $\nu C5\text{-}C6$, $\rho C1H_3$
3484	9254			9254		9	915(3)	916(8)	920(5)	ρNH_2, $\delta C4C3C2$, $\rho C6H_3$
3552	8633	454		8633		5	856(4)	855(9)	860(12)	ρNH_2,$\rho C6H_3$, $\nu_s C4\text{-}O8\text{-}C5$
3165	818	412		818	2	1	s.o.			$\rho C6H_3$, ρCH_2
3704	805	001		805	42	1	s.o.	786(36)	790(28)	$\gamma CH\alpha$, $\gamma C3C4O7$, $\rho C6H_3$, ρCH_2
3769	8	34					s.o.	752(8)		CO_2sci, ρNH_2, $\nu C2\text{-}CH_3$
3978	72	10		772	1	0	s.o.	752		γNH_2, $\gamma CH\alpha$
				728	7	9	s.o.	720(4)	725(1)	CO_2sci, ρCH_2
4026	685	291		685	28	1	655(6)*	675(br)	670(1)	γNH_2, Γ
4112	572	192		572	20	2	565(20)	567(14)	556(1)	$\gamma C2\text{-}C1H_3$
							515(5, br)	508(14)	520(5)	Intermolecular, $\gamma NH12$
4235	516	101		516	1	5				$\delta N\text{-}C\text{-}CH_3$
443	441	14		441	4	2	444(6)		450(4)	Δ, $\delta O\text{-}CH_2\text{-}CH_3$
	425	551					425(sh)	430(5)	415(5)	Δ, $\delta O\text{-}CH_2\text{-}CH_3$
4439	397	131		397	10	1	394(10)	395(8)	380(11)	$\nu N\cdots O$, $\delta C2\text{-}C1H_3$
4325	348	170							330(4)	$\delta C4\text{-}O8\text{-}C5$, $\delta C\text{-}C1H_3$
							330(7)	330(sh)		Δ, $\delta C4\text{-}O8\text{-}C5$, $\tau C6H_3$
46				332	5	3	330(9)	330(sh)		$\nu N\cdots O$, $\delta C2\text{-}C1H_3$
	270	331					275(5)		275(4)	γNH_{12},$\tau C6H3$

47	265	5	1					νN···O, τC6H3
48	247	7 1	4	250	97	4	275	γNH12, τC6H3
				238	2	0		τC6H3
49	177	4 2	2					γNH12, Γ, τC6H3
				171	6	0		τO-C2H5
50	127	3	0					δC-O-C2H5
				162	46	1		γNH12
51	121	16	1					Γ, τC1H3
				118	10	1		Γ, γC4O8
52	115	1	0	112	0	0		τC1H3
53	85	12	0	65	0	1		τO-C2H5
54	48	1	1	63	9	1		γO-C2H5

[a] Freq, vibrational wavenumber; I_{IR}, IR intensities in kM/mol; A_R, Raman scattering activities in A**4/AM; experimental relative intensities are given in parenthesis; br, broad; sh, shoulder; w, weak; v, very; s, symmetric; a, asymmetric υ, stretching; δ, in-plane bending; γ, out-of-plane bending; ρ, rocking inplane; π, rocking out-of-plane; ω, wagging; Δ, in-plane chelated ring deformation; τ, torsion; sci, scissoring; Γ, out-of-plane ring deformation; s.o., solvent overlapped;*, below 600 cm^{-1} obtained with different instrument.

Table 7. Experimental (FT-IR wavenumbers (in cm^{-1})) and theoretical (scaled wavenumbers (in cm^{-1})) of D3EAB at B3LYP/6-311++G(d,p) level of theory. [a]

No.	Theoretical						Experimental	Assignment
	AK1			AK2				
	Freq.	I_{IR}	A_R	Freq.	I_{IR}	A_R	IR(CCl_4)	
1	3134	11	50	3134	11	51	2980(50)	$\nu_a C1H_3$
2	3110	42	22	3125	29	8	2957(23)	$\nu_a CH_2$, $\nu_a C6H_3$
3	3099	31	94	3104	12	85	2932(21)	$\nu_a C6H_3$, $\nu_a CH_2$

4	3077	6	88	3093	30	107	2932	ν_aCH_2, ν_aC6H_3
5	3073	12	108	3074	13	107	2904(15)	ν_aC1H_3
6	3044	20	135	3065	33	150	2872(8)	ν_sCH_2
7	3033	23	188	3031	23	200	2801(4)	ν_sC6H_3
8	3025	29	277	3025	29	275	2729(2)	ν_sC1H_3
							2625(22)	νND_2free
9	2737	64	32	2737	64	32	2587(15)	ν_aND_2
10	2538	49	58	2539	48	58	2441(25)	ν_sND_2
11	2380	1	23	2380	1	24	2301(5)	$\nu CD\alpha$
12	1691	292	14	1691	269	13	1663(44)	$\nu_aO{=}C{-}C{=}C$, $\nu_aN{-}C{-}C{-}C$
13	1610	486	130	1610	496	130	1583(45)	$\nu_sO{=}C{-}C{=}C$, $\nu_sN{-}C{-}C{-}C$
14	1521	7	3				1480 (13)	$SciCH_2$, δ_aC6H_3
				1506	16	3	1468(9,sh)	δ_aC6H_3, $SciCH_2$
15	1499	4	11	1492	28	34	1444(17)	δ_aC6H_3, $SciCH_2$
16	1486	7	10	1487	12	23	1432(18)	δ_aC6H_3
17	1485	51	47	1484	36	27	1432	δ_aC1H_3
18	1482	9	8	1482	10	8	1432	δ_aC1H_3
19	1452	63	5	1450	55	3	1390(14)	$\nu_aCH_3{-}C{-}N$, $\delta sC1H_3$, $SciCH_2$
20	1424	3	2	1418	12	3	1375	δ_sC6H_3, $SciCH_2$
21	1409	1	4	1407	3	3	1375	δ_sC1H_3, δ_sC6H_3
22	1394	5	1	1397	11	2	1365(9)	ωCH_2, δ_sC6H_3
23	1294	1	10				1295(7, sh)	τCH_2
				1335	26	7	1274(90)	τCH_2
24	1278	758	9	1275	633	7	1256(90)	$\nu_aC3{-}C4{-}O8$, $\nu_aCH_3{-}C{-}N$, ωCH_2
25	1176	3	1				1161(64, sh)	$\rho C6H_3$, ρCH_2

				1194	26	2	1175(45)	ρC6H$_3$, ρCH$_2$
26	1167	26	7	1166	28	6	1135(10)	δND$_2$, δC=C-CH$_3$
27	1134	5	10					ρC6H$_3$,ν$_s$C6-C5-O8
				1116	119	3	1095(11)	ρC6H$_3$,ν$_a$C4-O8-C5
28	1105	271	0				1088(13)	ν$_a$C5-O8-C4, ρC1H$_3$, ρND$_2$
				1095	151	2	1065(31)	ν$_a$C5-O8-C4, ρC1H$_3$, ρND$_2$
29	1059	1	1	1059	2	1		ρC1H$_3$
30	1038	18	18	1029	21	5	1023(6)	ν$_a$C6-C5-O8, ρC1H$_3$
31	992	25	4				975(6)	ν$_s$C3-C4-O8, νC5-C6, ρC1H$_3$, δCDα
				976	26	5	965(5)	ν$_s$C3-C4-O8, νC5-C6, ρC1H$_3$, δCDα
32	952	7	11	950	3	13	942(4)	δND12, δC2C3C4
33	885	0	6	883	1	3		δCDα, ρND$_2$, ρC6H$_3$
34	877	3	4	867	2	6	865(20)	ρND$_2$, ν$_s$C4-O8-C5, ρC6H$_3$
35	822	0	3	823	0	3		ρND$_2$, δCDα, νC2-C1H$_3$
36	815	1	1	812	2	1		ρC6H$_3$, ρCH$_2$
37	791	23	0	794	23	0	670(5)	γC3C4O7, ρCH$_2$, ρC6H$_3$
38	748	3	5					CO$_2$sci, ρND$_2$, νC2-CH$_3$
				713	7	9	630(1)	CO$_2$sci, ρCH$_2$
39	589	2	3	592	2	4	587(1)	γC2-C1H$_3$, γCDα
40	571	4	1	574	4	0	560(2)	γCDα, γND$_2$
							536(2)	270 × 2 = 540 cm^{-1}
41				494	5	4	475(sh)	δN-C-CH$_3$, δC4-O8-C5
	480	17	2					γND10
42	468	11	3	478	21	0	450(5)	γND$_2$, γCDα
43				423	6	3	420(1)	Δ, δO-CH$_2$-CH$_3$
	408	4	2				410(1)	Δ, δO-CH$_2$-CH$_3$
44	390	13	1	392	11	1	390(br)	νN···O, δC-C1H$_3$
45	322	2	4					δC4-O8-C5, δC-C1H$_3$
				341	11	1		δC-C1H$_3$, τC6H$_3$, δC4-O8-C5
46	266	4	0					τC6H$_3$
				320	6	2		νN···O
47	255	6	1					νN···O, δC-C6H$_3$
				236	2	0		τC6H$_3$

48	222	29	2	218	32	2	Γ
49	151	31	1				γND_2, $\delta O\text{-}C2H_5$
				167	2	0	$\nu N\cdots O$, $\tau O\text{-}C_2H_5$
50	125	3	0				$\nu N\cdots O$, $\delta C\text{-}C6H_3$
				137	40	1	Γ, γND_2
51	118	23	1	117	16	2	Γ
52	114	0	0	111	0	0	$\tau C1H_3$
53	83	14	0	64	1	1	$\tau O\text{-}C_2H_5$
54	47	1	1	62	9	1	$\gamma O\text{-}C_2H_5$

[a] See footnote of Table 6.

Caption of the Figures:

Figure 1: The Tautomeric forms of β-Enaminones.

Figure 2: The optimized structures (the more stable aminoketone forms) of EAB at B3LYP/6-311++G(d,p) level, with the atom numbering.

Figure 3: Relative energy profile during the proton transfer process; a) EAB b) Bn-EAB (convert AK to IE).

Figure 4: The IR spectra of EAB (———) and its deuterated analogue (……) in CCl_4 solution: a) in the 1700–900 cm^{-1} range. b) in the 3600–2300 cm^{-1} range.

Figure 5: The IR spectra of EAB (———) and its deuterated analogue (……) in CCl_4 solution in the 700–250 cm^{-1}range.

Figure 6: The recorded Raman spectrum of EAB in liquid phase in the 1700–200 cm^{-1} range.

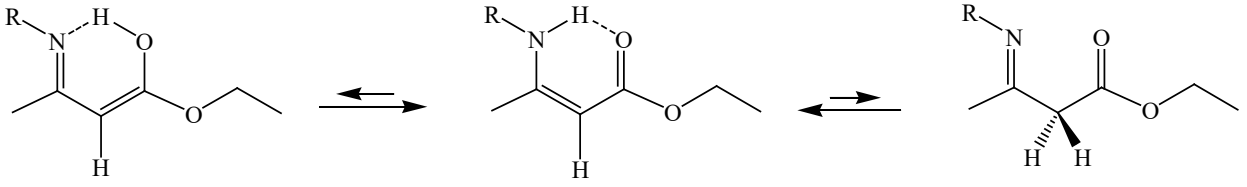

Iminoenol (IE) Aminoketone (AK) (chelated) Iminoketone (IK)

EAB: R=H
Me-EAB: R=Me
Ph-EAB: R=Ph
Be-EAB: R=CH_2-Ph

Figure 1.

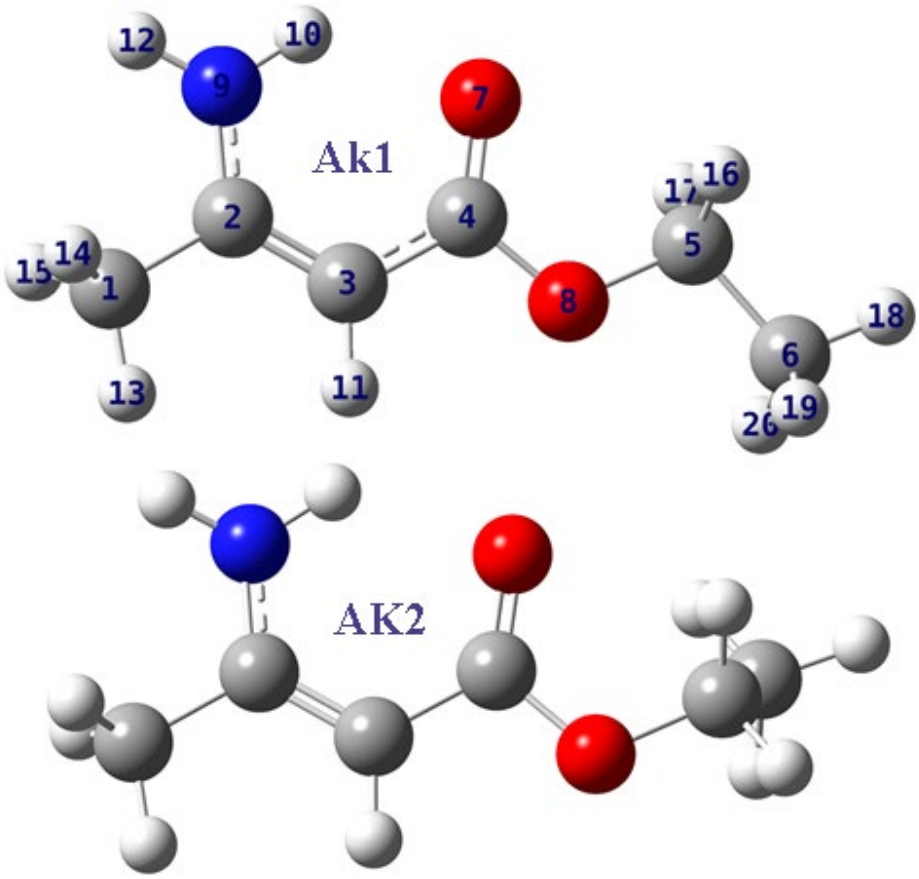

Figure 2.

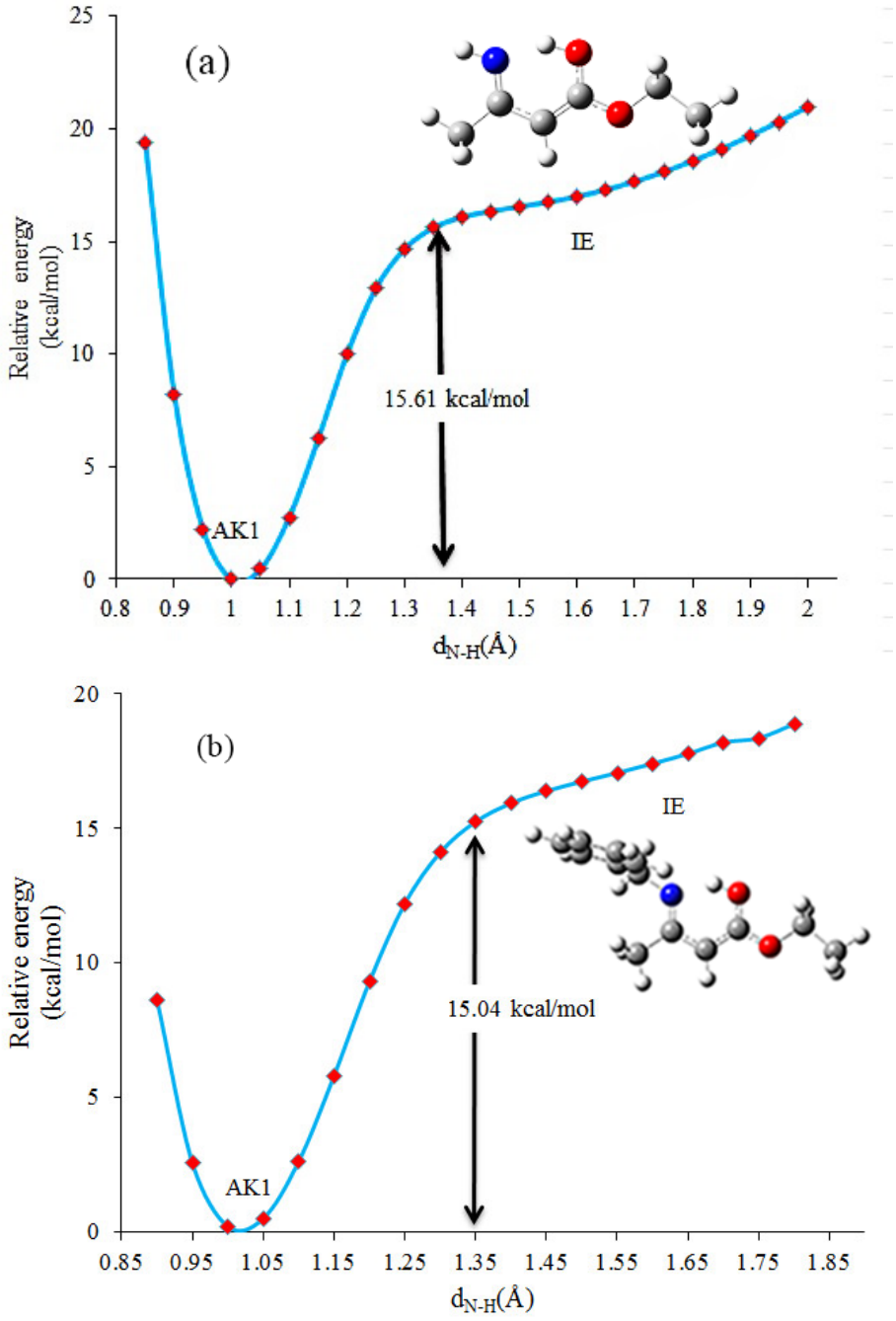
(a)
Relative energy (kcal/mol)
25
20
15
10
5
0
0.8 0.9 1 1.1 1.2 1.3 1.4 1.5 1.6 1.7 1.8 1.9 2
d_{N-H}(Å)
AK1
15.61 kcal/mol
IE
(b)
Relative energy (kcal/mol)
20
15
10
5
0
0.85 0.95 1.05 1.15 1.25 1.35 1.45 1.55 1.65 1.75 1.85
d_{N-H}(Å)
AK1
15.04 kcal/mol
IE

Figure 3.

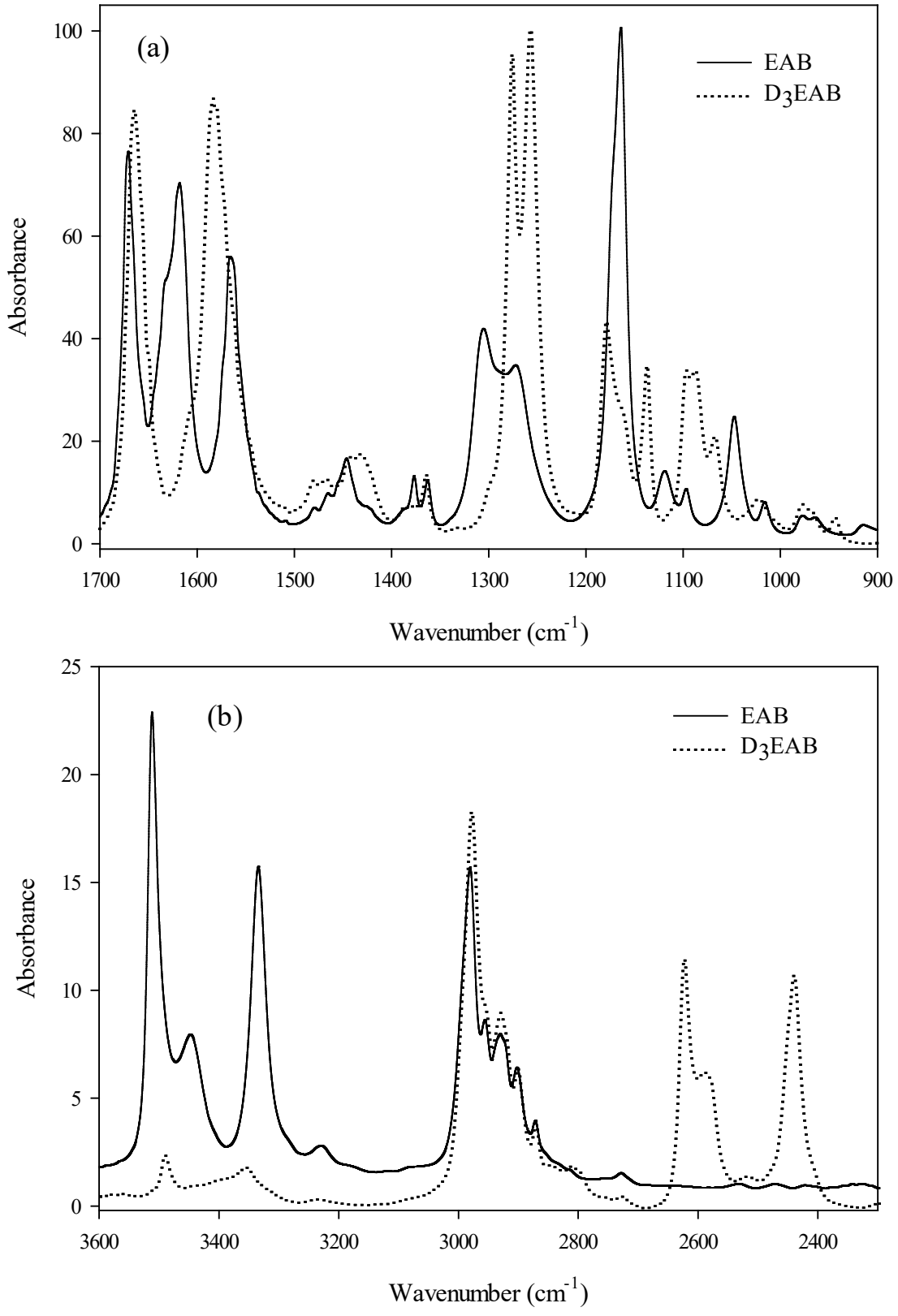
(a)
EAB
D3EAB
Absorbance
Wavenumber (cm-1)
(b)
EAB
D3EAB
Absorbance
Wavenumber (cm-1)

Figure 4.

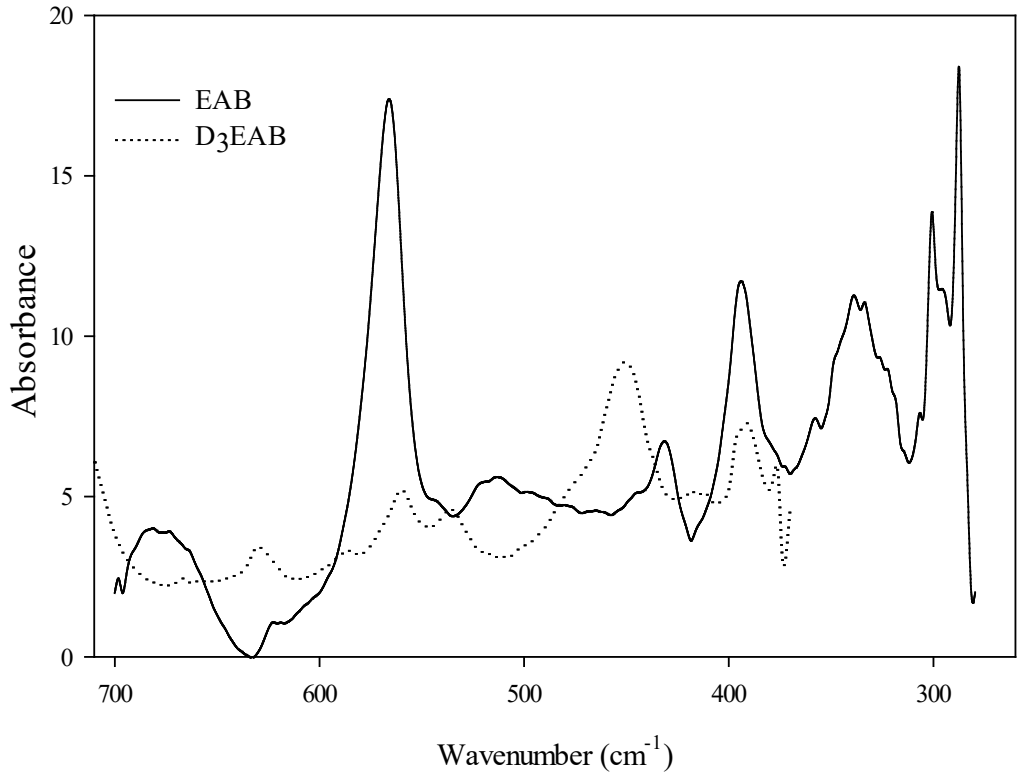
EAB
D3EAB
Absorbance
Wavenumber (cm-1)
20
15
10
5
0
700
600
500
400
300

Figure 5.

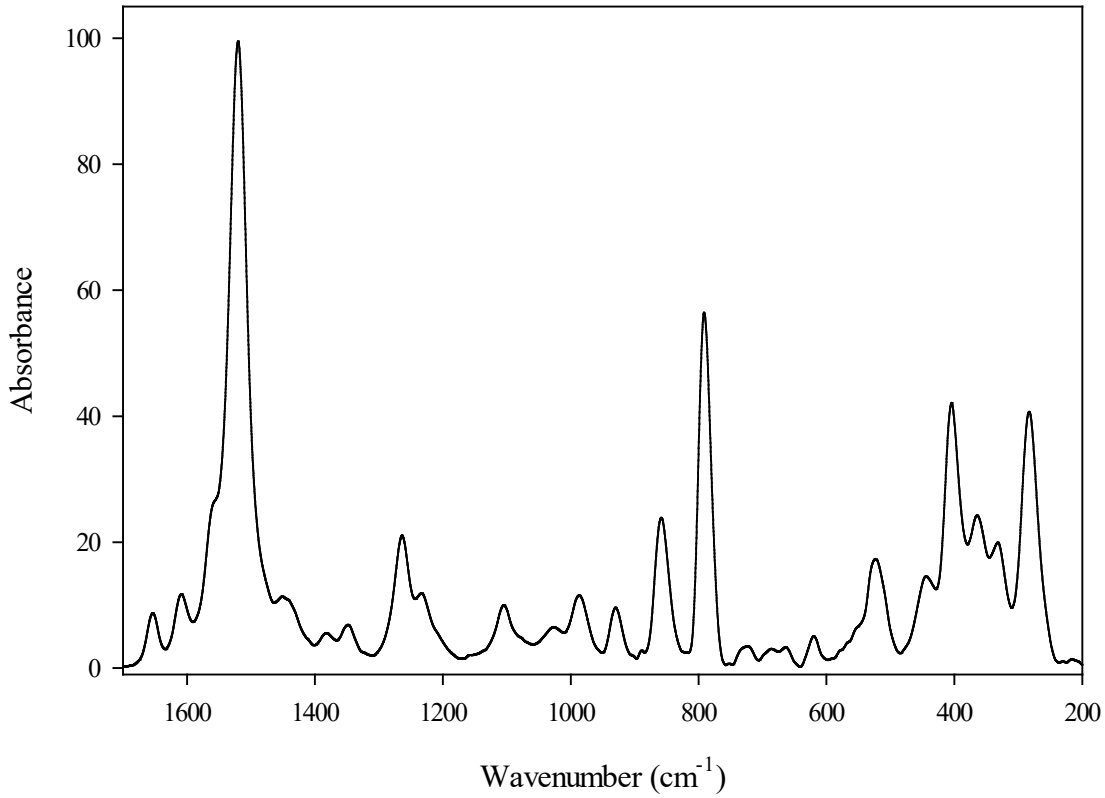
Absorbance
Wavenumber (cm-1)
100
80
60
40
20
0
1600
1400
1200
1000
800
600
400
200

Figure 6.

Supplementary material:

Table S1. Some selected parameters for both stable conformers of Me-EAB, Ph-EAB, and Bn-EAB calculated at B3LYP and MP2 levels with a 6-311++G(d,p) basis set.

Table S2. Values of the Fukui function considering natural charges according with Eqs. (1)–(3) for EAB, Me-EAB, Ph-EAB, and Bn-EAB obtained by B3LYP level with the 6-311++G(d,p) basis set.

Table S3. Experimental (FT-IR wavenumbers (in cm^{-1})) and theoretical (scaled wavenumbers (in cm^{-1})) of Ph-EAB at B3LYP/6-311++G(d,p) level of theory.[a]

Table S4. Experimental (FT-IR wavenumbers (in cm^{-1})) and theoretical (scaled wavenumbers (in cm^{-1})) of Bn-EAB at B3LYP/6-311++G(d,p) level of theory.[a]

Fig. S1. The possible stable forms in aminoketone tautomer of EAB (The relative energies in kcal mol^{-1}, which were calculated at B3LYP/6-311++G(d,p)). The values in parentheses were calculated at MP2/6-311++G(d,p).

Fig. S2. The most stable conformers of Me-EAB, Ph-EAB, and Bn-EAB.

Fig. S3. NMR spectra of EAB, Me-EAB, Me-EAB, Ph-EAB, and Bn-EAB in $CDCl_3$.

Fig. S4. Plot of ^{13}C chemical shifts vs. ^{13}C nuclear shielding.

Fig. S5. UV absorption spectra of EAB, Me-EAB, Ph-EAB, and Bn-EAB in ethanol solvent at a concentration of 2×10^{-3} M with a 10 mm quartz cell.

Fig. S6. The calculated HOMO-LUMO energy gaps for the EAB, Me- EAB, Ph-EAB, and Bn-EAB.

Fig. S7. MEP (left) and the point charges, electric potential values (right) on atoms of EAB, Me-EAB, Ph-EAB, and Bn-EAB.

Fig. S8. The deconvoluted IR spectra of EAB in the CCl_4 solution: a) in the 1700–900 cm^{-1} range. b) in the 3600–2800 cm^{-1} range.

Fig. S9. The recorded infrared spectra of EAB in the liquid phase (———) as well as MAB in the solid phase (……) (in the 3600–500 cm^{-1} range).

Fig. S10. The recorded infrared spectra of Me-EAB (———) and its deuterated analog (……) in CCl_4 solution: a) in the 1700–900 cm^{-1} range. b) in the 3400–2200 cm^{-1} range.

Fig. S11. The recorded infrared spectra of Ph-EAB (———) and its deuterated analog (……) in CCl_4 solution: a) in the 1700–900 cm^{-1} range. b) in the 3400–2200 cm^{-1} range.

Fig. S12. The recorded infrared spectra of Bn-EAB in CCl_4 solution (———) (in the 3500–800 cm^{-1} range).

Table S1.

	Me-EAB				Ph-EAB				Bn-EAB			
	B3LYP		MP2		B3LYP		MP2		B3LYP		MP2	
	AK1	AK2	AK1	AK2	AK1	AK2	AK1	AK2	AK1	AK2	AK1	AK2
Bond length (Å)												
C1-C2	1.505	1.505	1.505	1.505	1.506	1.506	1.506	1.506	1.505	1.505	1.504	1.504
C2=C3	1.376	1.376	1.375	1.375	1.374	1.374	1.374	1.375	1.375	1.375	1.371	1.372
C2-N	1.353	1.353	1.362	1.361	1.364	1.364	1.365	1.365	1.357	1.357	1.370	1.370
C3-C4	1.439	1.439	1.448	1.447	1.443	1.443	1.448	1.448	1.441	1.440	1.451	1.451
C4=O7	1.232	1.232	1.231	1.232	1.231	1.231	1.232	1.233	1.232	1.232	1.232	1.232
C4-O8	1.360	1.362	1.359	1.360	1.357	1.357	1.357	1.358	1.359	1.361	1.357	1.358
O8-C5	1.442	1.444	1.439	1.440	1.444	1.444	1.440	1.441	1.443	1.444	1.440	1.442
C5-C6	1.516	1.521	1.515	1.519	1.516	1.521	1.514	1.519	1.516	1.521	1.514	1.519
N-H10	1.017	1.017	1.018	1.018	1.022	1.022	1.022	1.021	1.018	1.018	1.019	1.019
N···O7	2.721	2.720	2.731	2.729	2.710	2.710	2.698	2.696	1.451	1.451	1.456	1.456
H10··· O7	1.913	1.911	1.453	1.452	1.869	1.869	1.878	1.877	2.721	2.723	2.738	2.736
Bond angles (°)												
C1C2C3	120.2	120.1	120.2	120.2	119.3	119.3	120.2	120.1	120.1	120.0	120.7	120.7
C1C2N	117.4	117.4	116.9	116.9	119.7	119.7	118.3	118.3	117.7	117.8	116.7	116.7
C2C3C4	122.7	122.7	122.3	122.4	123.4	123.4	122.4	122.5	122.8	122.9	122.5	122.5
C3C4O7	126.1	126.0	122.7	122.8	126.0	126.0	121.5	121.5	126.1	126.0	126.4	126.2
C3C2N	122.4	122.5	126.3	126.2	120.9	120.9	126.1	125.9	122.1	122.2	122.6	122.6
C3C4O8	112.4	112.3	111.8	111.6	112.4	112.4	111.9	111.8	112.4	112.2	111.7	111.5
C4O8C5	116.6	117.3	114.9	115.5	116.6	116.6	115.0	115.6	116.6	117.4	115.0	115.6
HNH (or C)	119.6	119.5	118.0	118.1	116.6	116.6	119.2	119.2	119.3	119.3	116.1	116.1
C2C3H11	119.4	119.4	119.5	119.5	119.1	119.1	119.4	119.3	119.3	119.3	119.6	119.6
NHO	134.1	134.2	134.7	134.7	137.2	137.2	134.9	134.9	134.7	134.5	136.4	136.3

Table S2

Atoms	EAB			Atoms	Me-EAB			Atoms	Ph-EAB			Atoms	Bn-EAB		
	f_k^+	f_k^-	f_k^0		f_k^+	f_k^-	f_k^0		f_k^+	f_k^-	f_k^0		f_k^+	f_k^-	f_k^0
C1	0.001	-0.298	-0.148	C1	0.282	0.021	0.151	C1	0.001	-0.298	-0.148	C1	0.295	-0.296	0
C2	-0.067	0.106	0.019	C2	-0.155	0.004	-0.076	C2	-0.067	0.106	0.019	C2	-0.157	0.108	-0.024
C3	-0.047	0.383	0.168	C3	0.213	-0.340	-0.063	C3	-0.047	0.383	0.168	C3	0.218	-0.112	0.053
C4	-0.032	-0.119	-0.076	C4	-0.393	0.039	-0.177	C4	-0.032	-0.119	-0.076	C4	-0.391	0.383	-0.004
C5	-0.002	-0.013	-0.008	C5	-0.055	0.077	0.011	C5	-0.002	-0.013	-0.008	C5	0.011	-0.011	0
C6	-0.012	-0.291	-0.152	C6	0.279	0.007	0.143	C6	-0.012	-0.291	-0.152	C6	0.28	-0.291	-0.006
O7	-0.042	-0.346	-0.194	O7	1.032	-0.094	0.469	O7	-0.042	-0.346	-0.194	O7	0.336	-0.351	-0.008
O8	-0.018	-0.286	-0.152	O8	0.278	-0.067	0.106	O8	-0.018	-0.286	-0.152	O8	0.281	-0.289	-0.004
N9	0.004	-0.232	-0.114	N9	0.301	-0.241	0.030	N9	0.004	-0.232	-0.114	N9	0.308	-0.234	0.037
H10	-0.008	0.210	0.101	H10	-0.225	-0.019	-0.122	H10	-0.008	0.210	0.101	H10	-0.224	0.205	-0.01
H11	-0.016	0.091	0.037	H11	-0.121	-0.031	-0.076	H11	-0.016	0.091	0.037	H11	-0.12	0.089	-0.016
H12	-0.043	0.094	0.026	H12	0.144	0.037	0.091	C12	-0.043	0.094	0.026	C12	0.08	-0.087	-0.004
H13	-0.013	-0.093	-0.053	H13	-0.168	-0.024	-0.096	C13	-0.013	-0.093	-0.053	C13	0.021	0.007	0.014
H14	-0.035	-0.117	-0.076	H14	-0.207	-0.035	-0.121	C14	-0.035	-0.117	-0.076	C14	0.098	-0.099	0
H15	-0.072	-0.092	-0.082	H15	-0.222	-0.038	-0.130	C15	-0.072	-0.092	-0.082	C15	0.086	-0.107	-0.011
H16	-0.015	-0.117	-0.066	H16	-0.107	-0.021	-0.064	C16	-0.015	-0.117	-0.066	C16	0.085	-0.102	-0.009
H17	-0.039	-0.090	-0.065	H17	-0.112	-0.021	-0.066	C17	-0.039	-0.090	-0.065	C17	0.093	-0.112	-0.009
H18	-0.078	0.094	0.008	H18	-0.193	-0.024	-0.109	H18	-0.078	0.094	0.008	C18	0.078	-0.106	-0.014
H19	-0.017	0.099	0.041	H19	-0.138	-0.011	-0.074	H19	-0.017	0.099	0.041	H19	-0.172	0.09	-0.041
H20	-0.015	0.100	0.043	H20	-0.141	-0.011	-0.076	H20	-0.015	0.100	0.043	H20	-0.144	0.095	-0.024
				H21	-0.194	-0.037	-0.115	H21	-0.015	0.084	0.034	H21	-0.146	0.1	-0.023
				H22	-0.250	-0.042	-0.146	H22	-0.007	0.084	0.039	H22	-0.112	0.083	-0.015
				H23	-0.218	-0.063	-0.140	H23	-0.107	0.091	-0.008	H23	-0.106	0.083	-0.012
								H24	-0.035	0.097	0.031	H24	-0.183	0.09	-0.047

H25	-0.019	0.097	0.039	H25	-0.14	0.097	-0.022
H26	-0.029	0.097	0.034	H26	-0.136	0.096	-0.02
H27	-0.115	0.091	-0.012	H27	-0.138	0.096	-0.021
H28	-0.061	0.089	0.014	H28	-0.173	0.09	-0.042
H29	-0.031	0.091	0.030	H29	-0.119	0.114	-0.003
H30	-0.013	0.098	0.042	H30	-0.252	0.093	-0.079
				H31	-0.137	0.095	-0.021
				H32	-0.238	0.092	-0.073

Table S3

No.	Theoretical AK1		Theoretical AK2		Experimental	
	Freq.	I_{IR}	Freq.	I_{IR}	IR(CCl_4)	Assignment
1	3256	189	3257	187	3265(m,br)	νNH
2	3094	1	3095	1	3197(w)	νCH(α)
3	3084	6	3086	6	3120(vw)	νCH(ph)
4	3067	18	3067	18	3097(vw)	νCH(ph)
5	3057	15	3057	15	3065(w)	νCH(ph)
6	3047	4	3047	4		νCH(ph)
7	3040	4	3040	4	3045(w)	νCH(ph)
8	3009	16	3010	15	2985(vw)	ν_aC1H_3
9			3004	30	2960(m)	ν_aC6H_3, ν_aC5H_2
	299	41			2937(vw)	ν_aC6H_3, ν_aC5H_2
10	2979	29	2984	11		ν_aC6H_3, ν_aC5H_2

11			2977	8	2905(w)	ν_aC6H_3
	2978	8				ν_aC1H_3
12			2973	30	2877(w)	ν_aC1H_3
	2959	5			2860(vw)	ν_aC5H_2, ν_aC6H_3
13	2927	18	2946	36		ν_SC5H_2
14			2923	11		ν_sC5H_2
	2924	11				ν_sC1H_3
15	2915	26	2913	25		ν_sC6H_3
16	1660	236	1659	208	1656(s)	ν_aO=C-C=C, ν_aN-C=C-C, δCH(α)
17	1643	592	1643	601	1620(s)	δNH, ν_sO=C-C=C, ν_sN-C=C-C
18	1617	214	1616	212	1598(s)	ν_aCC(ph)
19	1595	107	1595	114	1585(w,sh)	ν_aCC(ph)
20	1521	64	1521	64	1505(m)	ν_sN-C=C-C, δCH11, δNH, sci$C5H_2$,
21	1502	45	1500	116	1490(m)	δ_aCH(ph), sci$C5H_2$,δ_aC6H_3
22	1497	66			1490	δ_aCH(ph), sci$C5H_2$,δ_aC6H_2
			1485	6		δ_aCH(ph), sci$C5H_2$,δ_aC6H_3
23	1478	4	1472	12		sci$C5H_2$,δ_aC6H_3
24	1472	17	1468	11		sci$C5H_2$,δ_aC1H_3, δNH
25	1466	26	1465	13	1440(m)	sci$C5H_2$,δ_aC1H_3, δcH(α)
26	1465	7	1465	24	1440	δ_aC6H_3
27	1453	20	1452	16	1440	δ_aCH(ph), δ_aC1H_3,ν_aN-C=C-C, δCH(α),
28	1404	0				δ_sC1H_3, δ_sC6H_3, ω$C5H_2$
			1401	112	1385(w)	δ_sC1H_3, δNH
29	1402	121			1385	δ_sC1H_3, δ_sC6H_3, ω$C5H_2$, δNH
			1397	9	1385	δ_sC6H_3, ω$C5H_2$
30	1383	90	1383	9	1385	δ_sC1H_3, δNH, ν_sC-N-C,δ_sC6H_3
31	1375	33	1375	97	1360(w)	δ_sC1H_3, δNH, ν_sC-N-C, δ_sC6H_3, ω$C5H_2$
32	1338	14	1337	16	1300(vw)	δNH, ν_sC3=C2-N, δ_sCH(ph), δs$C1H_3$

33	1311	4	1314	39	1300	ν_sC3=C2-N, δ_sCH(ph), δsC1H$_3$, ωC5H$_2$
34	1284	704	1311	1	1270(s)	δcH(α), ν_sC3=C2-N, δ_sCH(ph), δ_sC1H$_3$, ωC5H$_2$
35	1276	1	1285	595	1270	τC5H$_2$, πCH$_3$
36	1237	220	1235	171	1235(s)	ν_aC3-C4-O8, ν_aC1-C2-N-C12, δCH(α)
37	1186	2	1185	3		τC5H$_2$, πCH$_3$
38	1168	544	1177	90	1165(s)	ν_aC3-C4-O8, ν_aC1-C2-N-C12, δCH(α)
39	1165	10	1166	411	1165	δ_aCH(ph)
40	1159	3	1165	43	1165	ρC5H$_2$, ρC6H$_3$
			1123	127		νN-CH$_2$, δC=C-N, ν_aC-O-CH$_2$, δCH(α), δ_aCH(ph)
41	1118	5				δO-CH$_2$-CH$_3$, ρC6H$_3$, νCH$_2$-O
			1099	68	1095(vw)	ρC6H$_3$, ν_aOCH$_2$-CH$_3$
42	1090	8	1090	6		δ_aCH(ph)
43	1065	90	1058	58	1058(w)	ν_aOCH$_2$-CH$_3$, ν_aC-C-O-CH$_2$, ρC1H$_3$
44	1043	4	1042	4		πC1H$_3$
45	1035	18	1035	15	1025(vw)	δCCC(ph), πC1H$_3$
46	1023	52	1017	58	1018(w)	ρC1H$_3$, ν_aO-CH$_2$-CH$_3$
47	1001	0	1001	0		ρC1H$_3$, ν_aO-CH$_2$-CH$_3$
48	982	1				γCH(ph), νC2-C1H$_3$, νC5-C6H$_3$, ν_sC3-C4-O8
			981	0		γCH(ph), ρC1H$_3$, πC12H$_2$
49	980	31			975(vw)	γCH(ph), ρC1H$_3$, δC2C3C4, νC5-C6H$_3$, ν_sC3-C4-O9
			964	0		γCH(ph)
50	966	0				γCH(ph)
			962	22	960(vw)	ρC1H$_3$, δC2C3C4, νC5-C6H$_3$, ν_sC3-C4-O9
51	953	2	933	7	940(w)	γCH(ph), πC12H$_2$
52	903	5	901	5	900(vw)	γCH(ph),
53	870	2	860	2	870(w)	ν_aOCH$_2$-CH$_3$, ν_aC-C-O-CH$_2$
54	831	2	829	2		Δ, ρC6H$_3$, ν_sC1H$_3$-C2-N, νO8-C5
53	809	3	811	3		ρC6H$_3$, ρC5H$_2$, Γ

54	791	64	794	64	γCH_2, πCH_3

[a] See footnote of Table 6.

Table S4

No.	Theoretical AK1		Theoretical AK2		Experimental	
	Freq.	I_{IR}	Freq.	I_{IR}	IR(CCl_4)	Assignment
1	3326	124	3329	122	3450(vw)	νNH
2	3094	1	3096	1	3290(m,br.)	νCH(α)
3	3065	14	3065	14	3207(w)	νCH(ph)
4	3058	19	3058	19	3115(vw)	νCH(ph)
5	3049	13	3049	13	3095(w)	νCH(ph)
6	3040	0	3040	0	3070(w)	νCH(ph)
7	3025	9	3025	9		νCH(ph)
8	3012	13	3012	12	3035(w)	$\nu_a C1H_3$
9			3003	31	2993(vw)	$\nu_a C6H_3$, $\nu_a C5H_2$
	2988	41			2950(m)	$\nu_a C6H_3$, $\nu_a C5H_2$
10	2978	31	2983	12	2930(vw)	$\nu_a C6H_3$, $\nu_a C5H_2$
11			2971	29		$\nu_a C6H_3$
	2962	7			2910(w)	$\nu_a C1H_3$
12			2963	29		$\nu_a C1H_3$
	2957	6			2870(w)	$\nu_a C1H_2$, $\nu_a C6H_3$
13	2945	14	2945	13	2885(vw)	$\nu_a C12H_2$
14			2944	35		$\nu_s C5H_2$
	2924	20				$\nu_s C5H_2$
15	2916	33	2915	37		$\nu_s C1H_3$, $\nu_s C12H_2$

16	2915	31	2912	26		$\nu_s C6H_3$
17	2912	6	2912	7	2840(w)	$\nu_s C1H_3$, $\nu_s C12H_2$
18	1659	326	1660	292	1660(s)	$\nu_a O{=}C{-}C{=}C$, $\nu_a N{-}C{=}C{-}C$, $\delta CH(\alpha)$
19	1632	568	1634	585	1613(s)	δNH, $\nu_s O{=}C{-}C{=}C$, $\nu_s N{-}C{=}C{-}C$
20	1620	14	1620	14	1613	$\nu_a CC(ph)$
21	1601	4	1601	4	1588(sh)	$\nu_a CC(ph)$
22	1513	83	1512	97	1500(m)	$\nu_s N{-}C{=}C{-}C$, $\delta CH(\alpha)$, δNH, $sciC5H_2$, $sciC12H_2$
23	1503	10	1503	12	1496(m)	$\delta_a CH(ph)$, $sciC12H_2$
24	1498	10	1485	5	1496	$sciC5H_2$,$\delta_a C6H_3$
25	1476	29	1478	29	1460(m)	$\delta_a C1H_3$, $sciC12H_2$, δNH
26	1477	4	1470	11	1460	$sciC5H_2$,$\delta_a C1H_3$, δNH
27	1468	14	1467	7	1440(m)	$\delta_a C1H_3$, $sciC12H_2$
28	1465	7	1465	9	1440	$\delta_a C6H_3$
29	1461	10	1461	12	1433(sh)	$\delta_a CH(ph)$, $\delta_a C1H_3$, $\omega C12H_2$
30	1458	23	1458	19	1433	$\delta_a C1H_3$, $sciC12H_2$
31	1404	6				$\delta_s C1H_3$, $\delta_s C6H_3$, $\omega C5H_2$
			1403	77	1387(m)	$\delta_s C1H_3$, δNH
32	1402	71			1387	$\delta_s C1H_3$, $\delta_s C6H_3$, $\omega C5H_2$, δNH
			1398	10	1370(vw)	$\delta_s C6H_3$, $\omega C5H_2$
33	1384	15	1386	15	1370	$\delta_s C1H_3$, δNH, $\omega C12H_2$, $\nu_s C{-}N{-}C$
34	1375	2	1378	15	1360(w)	$\delta_s C6H_3$, $\omega C5H_2$
35	1359	83	1359	81	1340(vw)	$\omega C12H_2$, δNH, $\nu_s C3{=}C2{-}N$, $\delta_s CH(ph)$, $\delta sC1H_3$
36	1333	3	1333	3	1350(w)	$\delta_s CH(ph)$, $\omega C12H_2$
37			1315	76	1310(sh)	$\omega C5H_2$
38	1312	151			1310	$\tau C12H_2$, $\omega C5H_2$, $\delta CH(\alpha)$, $\nu_a C{-}C(ph)$
			1312	75	1310	$\tau C12H_2$, $\tau C5H_2$, $\delta CH(\alpha)$, $\nu_a C{-}C(ph)$
39	1290	133	1290	132	1280(m)	$\nu_a C{-}C(ph)$, $\tau C12H_2$, $\delta CH(\alpha)$
40	1276	0				$\tau C5H_2$, πCH_3

			1289	132	1280	τC5H_2, ν_aC3-C4-O8, ν_aC1-C2-N-C12
41	1246	476	1243	386	1234(s)	τC12H_2, ν_aC3-C4-O8, ν_aC1-C2-N-C12, δCH(α)
42	1195	56	1195	41	1199(w)	ν_aC13-C12-N, ν_aC3-C4-O8, δCH7
43	1184	12	1185	8	1190(w)	δ_aCH(ph), δCH(α)
44			1178	116	1173(s)	ρC5H_2, ρC6H_3
	1174	311			1173	δCH(α), ν_sN-C12-C13, ν_aC-O-CH_2
45			1172	194	1173	δCH(α), ν_sN-C12-C13, ν_aC-O-CH_2
	1164	0			1173	δ_aCH(ph)
46			1165	0		δ_aCH(ph)
	1159	3			1150(m)	ρC5H_2, ρC6H_3
47	1125	90			1121(m)	νN-CH_2, δC=C-N, ρC6H_3, ν_aC-O-CH_2, δCH(α), δ_aCH(ph)
			1123	127	1120	νN-CH_2, δC=C-N, ν_aC-O-CH_2, δCH(α), δ_aCH(ph)
48	1116	36			1120	δO-CH_2-CH_3, ρC6H_3, νCH_2-N
	0		1099	58	1105(vw)	ρC6H_3, ν_aOCH_2-CH_3
49	1083	23	1084	17	1075(w)	δ_aCH(ph), νCH_2-N
50	1065	75	1059	45	1060(w)	ν_aOCH_2-CH_3, ν_aC-C-O-CH_2, ρC1H_3
51	1045	4	1046	3		πC1H_3
52	1033	13	1033	13	1030(vw)	δCCC(ph)
53	1027	50	1022	59	1015(w)	ρC1H_3, ν_aO-CH_2-CH_3, πC12H_2
54	1002	1	1002	1	1002(vw,sh)	δCCC(ph)
55	991	2	991	1		γCH(ph), πC12H_2
56	984	14			982(vw)	γCH(ph), νC2-C1H_3, νC5-C6H_3, ν_sC3-C4-O8
			981	2		γCH(ph), ρC1H_3, πC12H_2
57	976	12			977(vw)	γCH(ph), ρC1H_3, δC2C3C4, νC5-C6H_3, ν_sC3-C4-O9, πC12H_2
			972	0		γCH(ph)
58	971	0				γCH(ph)
			961	21	935(m)	ρC1H_3, δC2C3C4, νC5-C6H_3, ν_sC3-C4-O9
59	904	2	904	2	900(vw)	γCH(ph), πC12H_2

60	885	1	877	0		γCH(ph), ρC6H$_3$, δC3C4O8, ν$_s$C4-O8-C5, πC12H$_2$
61	845	0	846	1		γCH(ph)
62	831	7	828	6		Δ, ρC6H$_3$, ν$_s$C1H$_3$-C2-N, νO8-C5
63	803	3	806	2	845(w)	ρC6H$_3$, ρC5H$_2$, Γ
64	792	3	793	3		δCCC(ph), νC12-C13, γNH

[a] See footnote of Table 6.

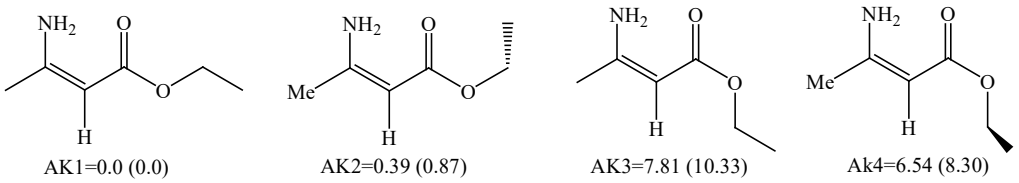
NH2
O
O
H
AK1=0.0 (0.0)
NH2
O
Me
O
H
AK2=0.39 (0.87)
NH2
O
O
H
AK3=7.81 (10.33)
NH2
O
Me
O
H
Ak4=6.54 (8.30)

Fig. S1.

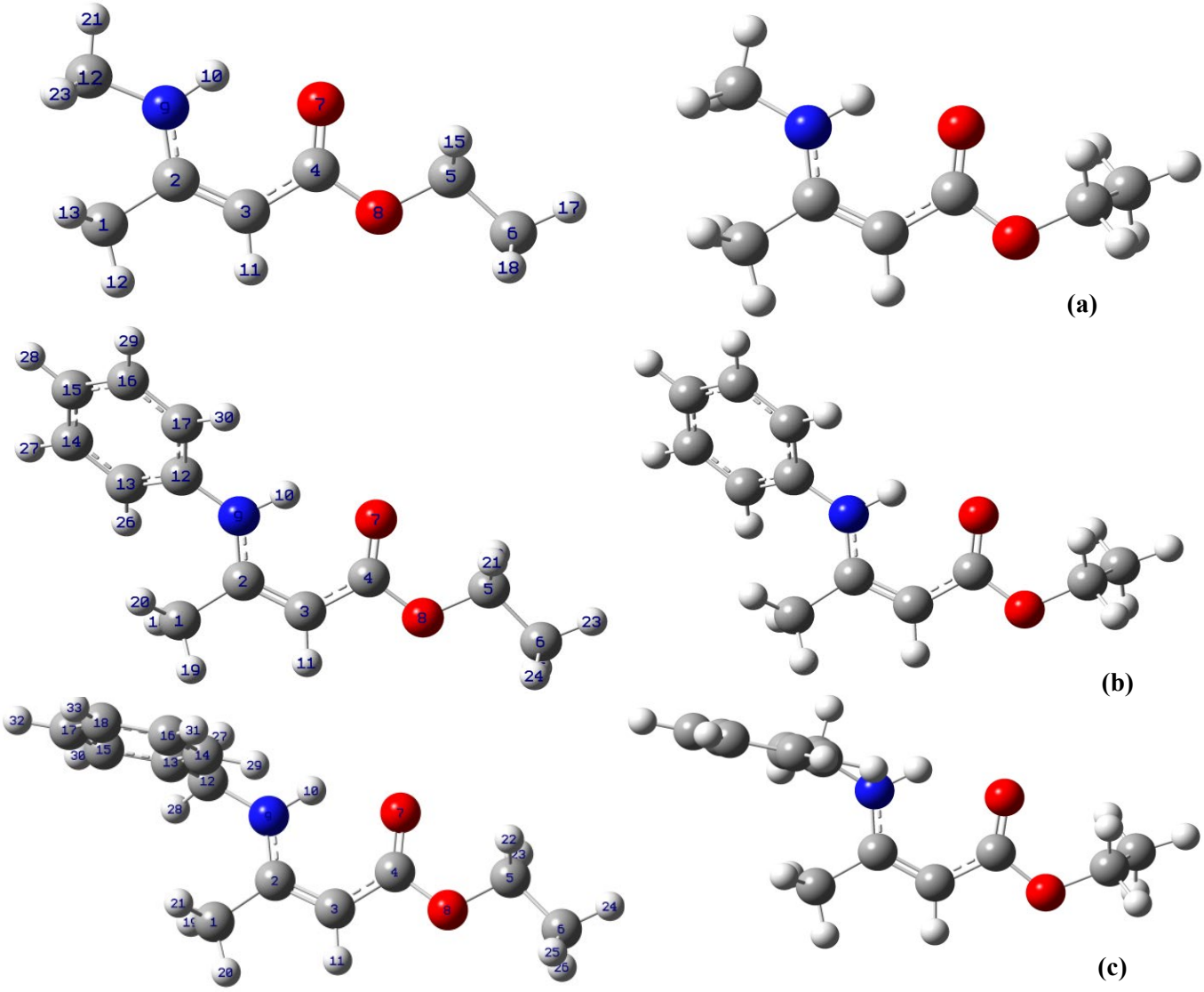
(a)
(b)
(c)

Fig. S2.

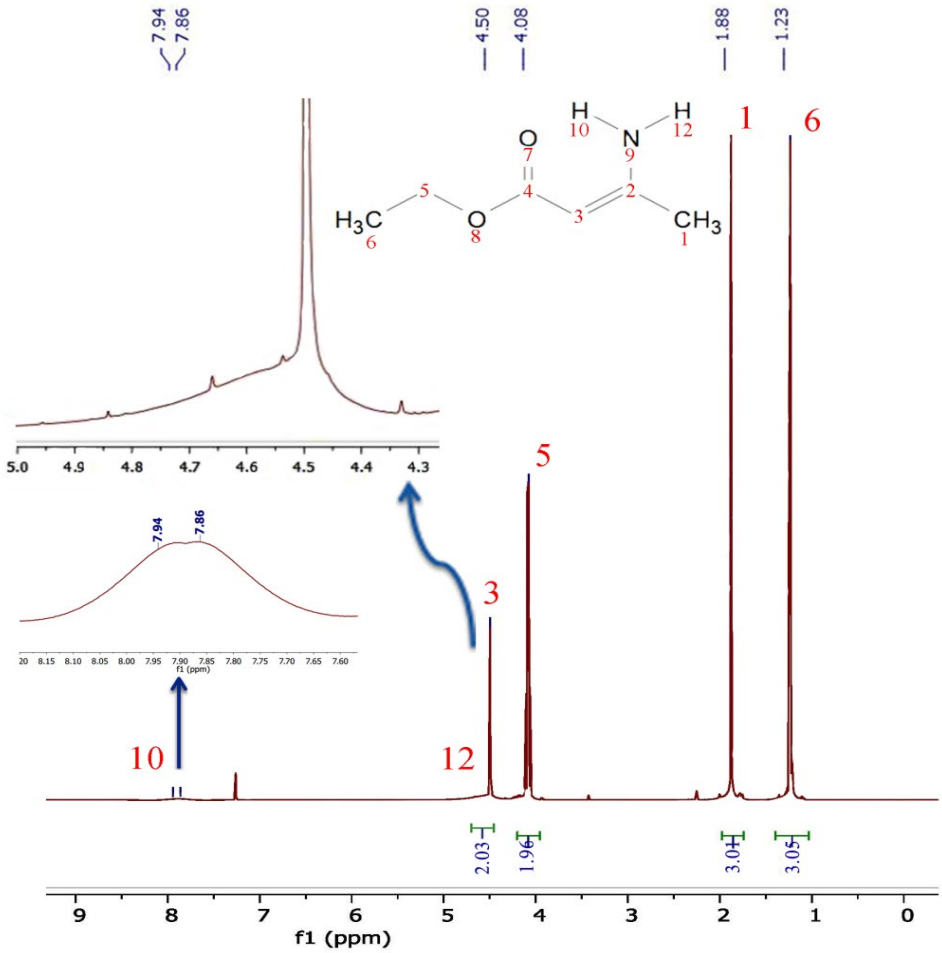
7.94
7.86
4.50
4.08
1.88
1.23
H
10
N
9
H
12
O
7
4
2
3
5
O
8
H_3C
6
CH_3
1
1
6
5
3
12
10
2.03
1.96
3.04
3.05
9
8
7
6
5
4
3
2
1
0
f1 (ppm)

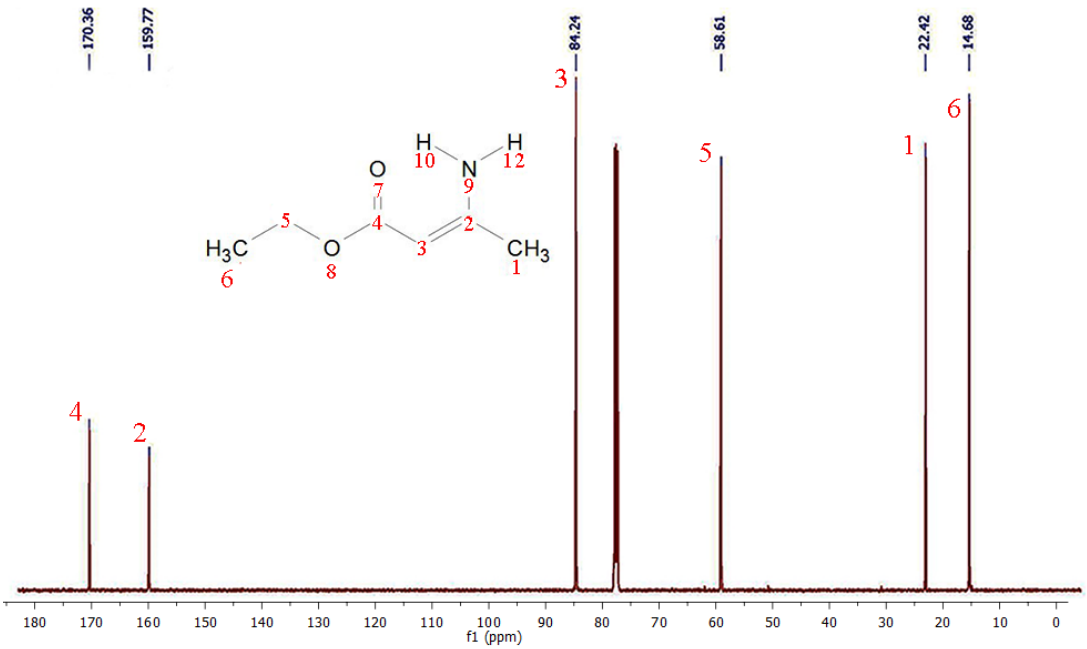
170.36
159.77
84.24
58.61
22.42
14.68
f1 (ppm)

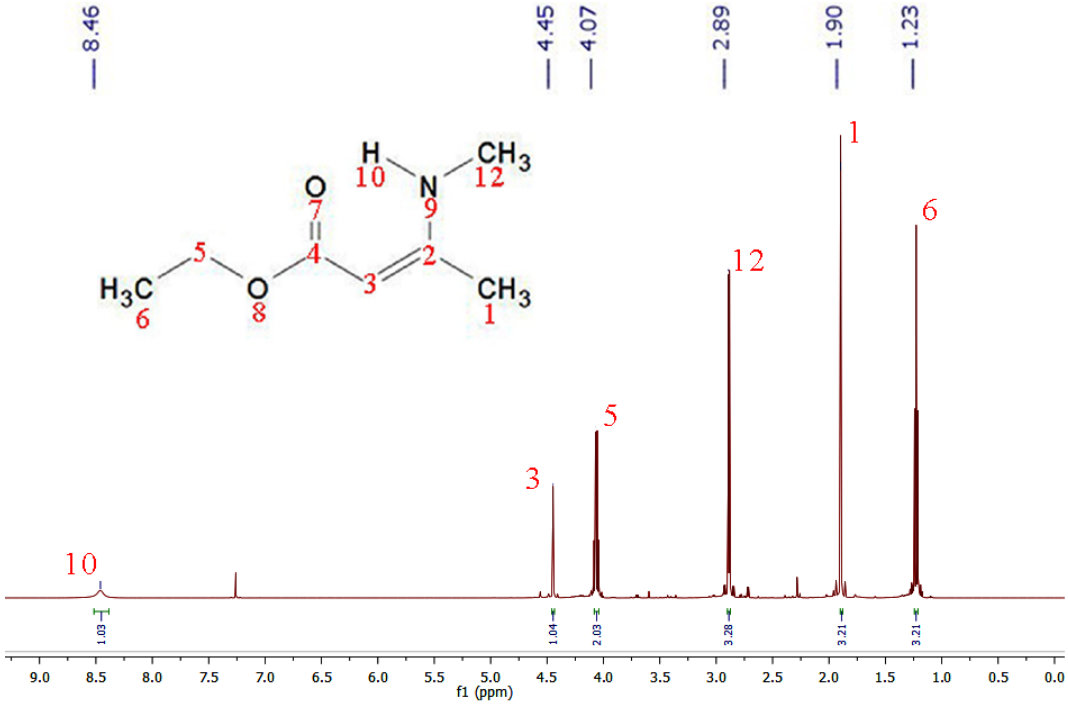
8.46
4.45
4.07
2.89
1.90
1.23
1.03
1.04
2.03
3.28
3.21
3.21
f1 (ppm)

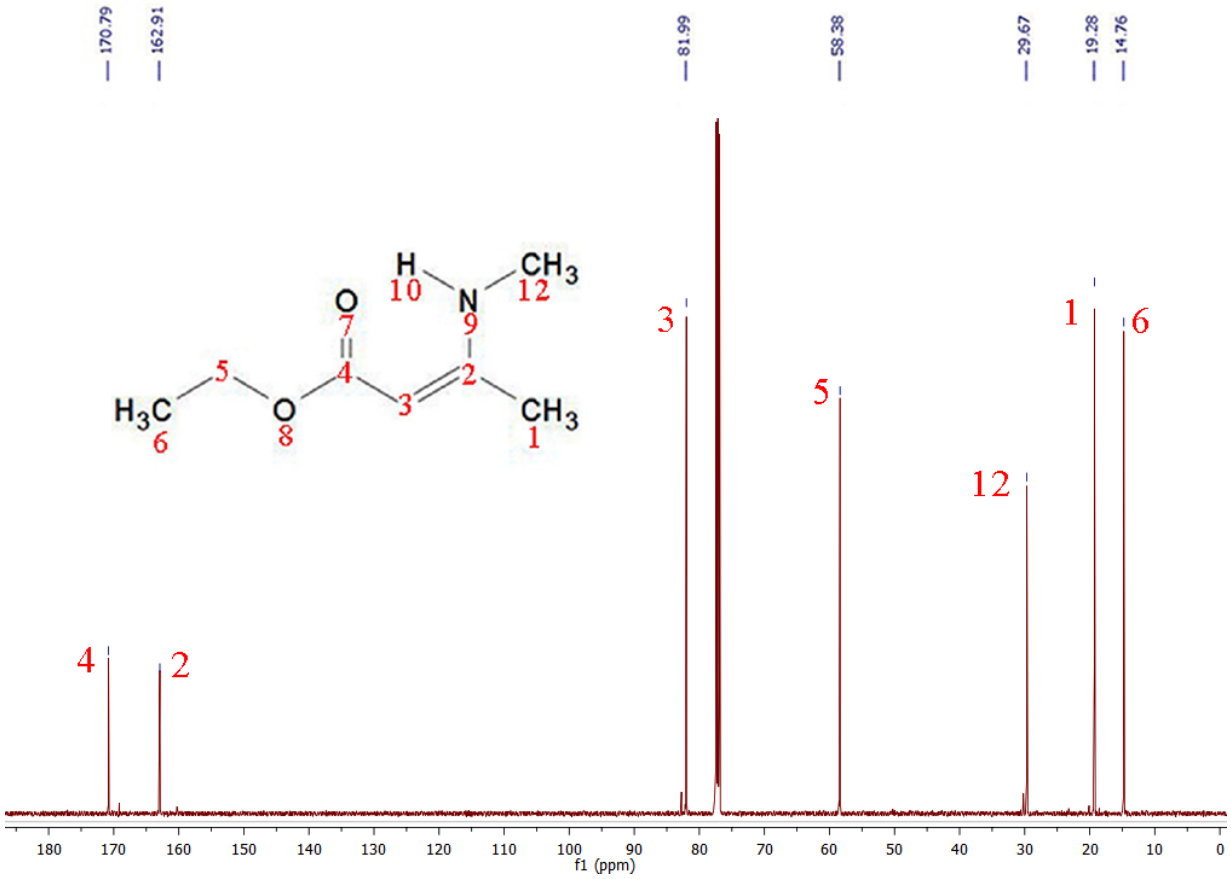
170.79
162.91
81.99
58.38
29.67
19.28
14.76
H
10
N
12
CH3
O
7
4
5
3
2
H3C
6
O
8
CH3
1
3
5
1
6
12
4
2
180 170 160 150 140 130 120 110 100 90 80 70 60 50 40 30 20 10 0
f1 (ppm)

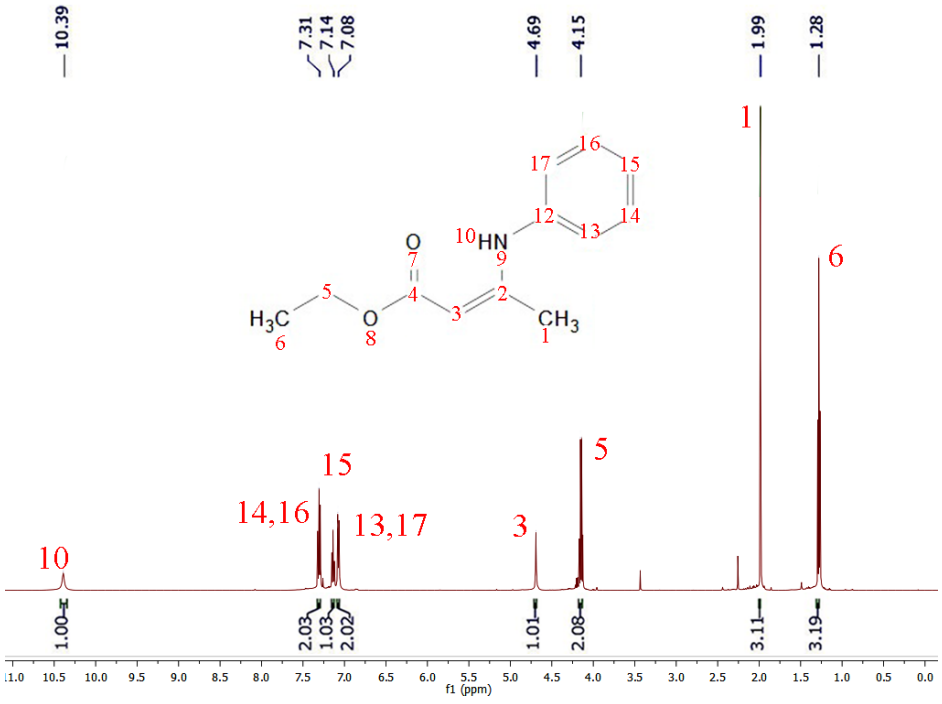
10.39
7.31
7.14
7.08
4.69
4.15
1.99
1.28
16
17
15
12
13
14
10HN
9
O
7
4
5
3
2
H3C
6
O
8
CH3
1
1
6
5
15
14,16
13,17
3
10
1.00
2.03
1.03
2.02
1.01
2.08
3.11
3.19
f1 (ppm)

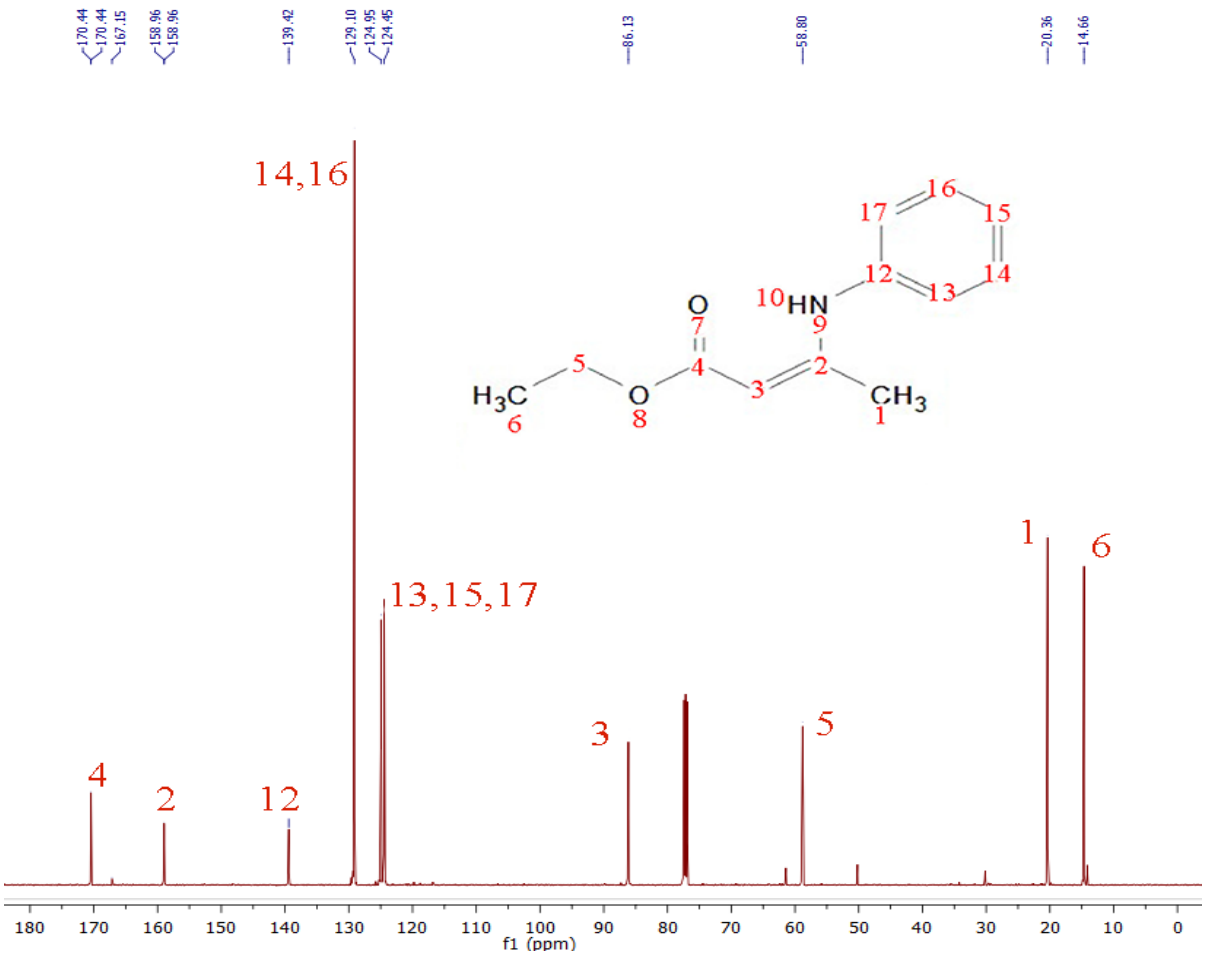
170.44
170.44
167.15
158.96
158.96
139.42
129.10
124.95
124.45
86.13
58.80
20.36
14.66
14,16
13,15,17
4
2
12
3
5
1
6
180
170
160
150
140
130
120
110
100
90
80
70
60
50
40
30
20
10
0
f1 (ppm)

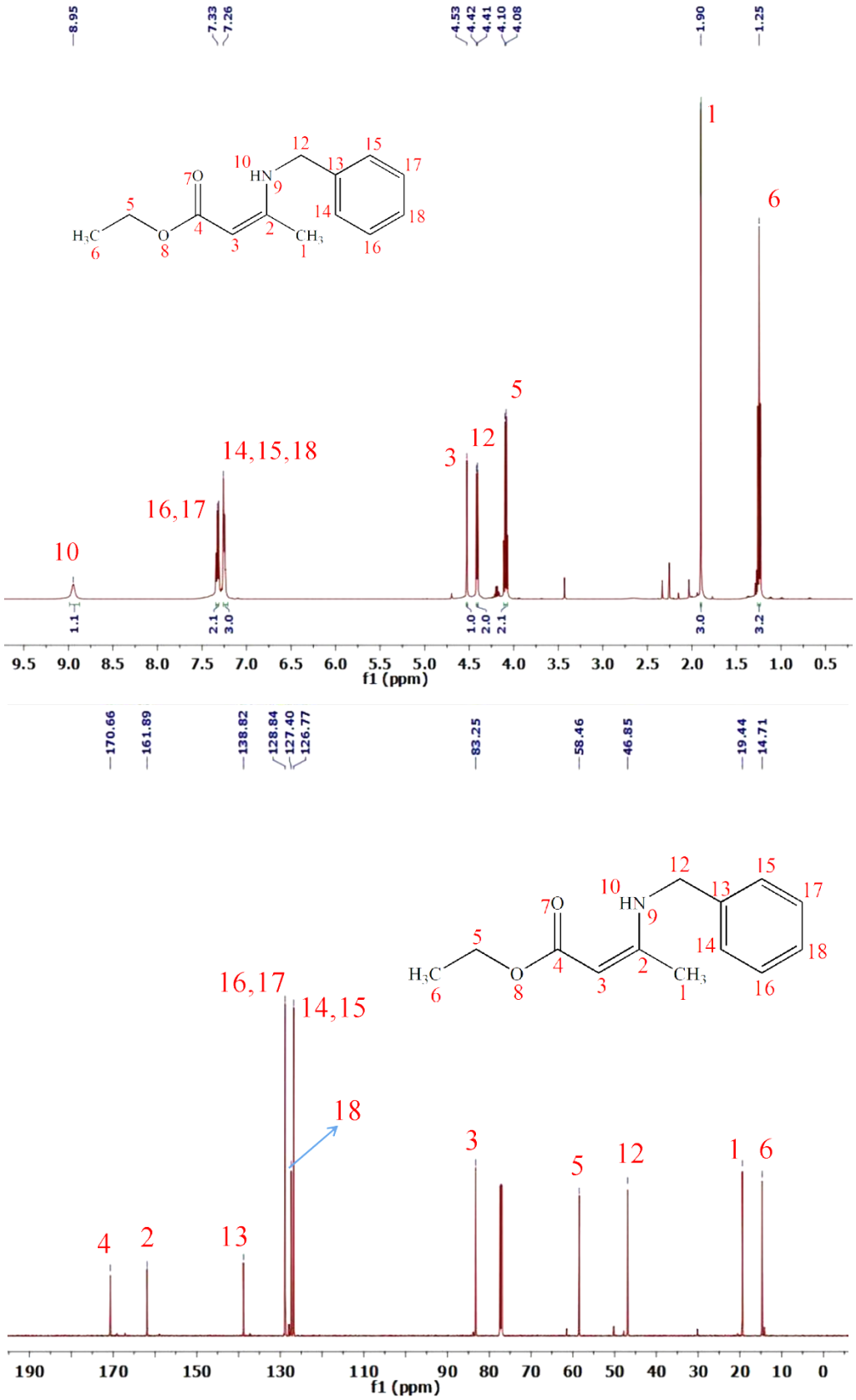
8.95
7.33
7.26
4.53
4.42
4.41
4.10
4.08
1.90
1.25
1
6
5
12
3
14,15,18
16,17
10
1.1
2.1
3.0
1.0
2.0
2.1
3.0
3.2
9.5 9.0 8.5 8.0 7.5 7.0 6.5 6.0 5.5 5.0 4.5 4.0 3.5 3.0 2.5 2.0 1.5 1.0 0.5
f1 (ppm)
170.66
161.89
138.82
128.84
127.40
126.77
83.25
58.46
46.85
19.44
14.71
16,17
14,15
18
3
5
12
1
6
4
2
13
190 170 150 130 110 90 80 70 60 50 40 30 20 10 0
f1 (ppm)

Fig. S3.

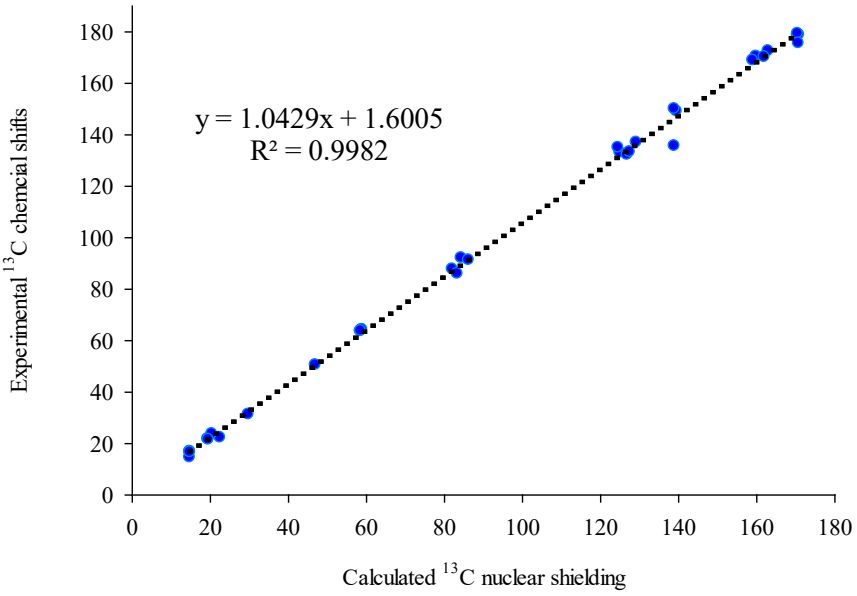
y = 1.0429x + 1.6005
R² = 0.9982
Experimental ^{13}C chemcial shifts
Calculated ^{13}C nuclear shielding
0
20
40
60
80
100
120
140
160
180

Fig. S4.

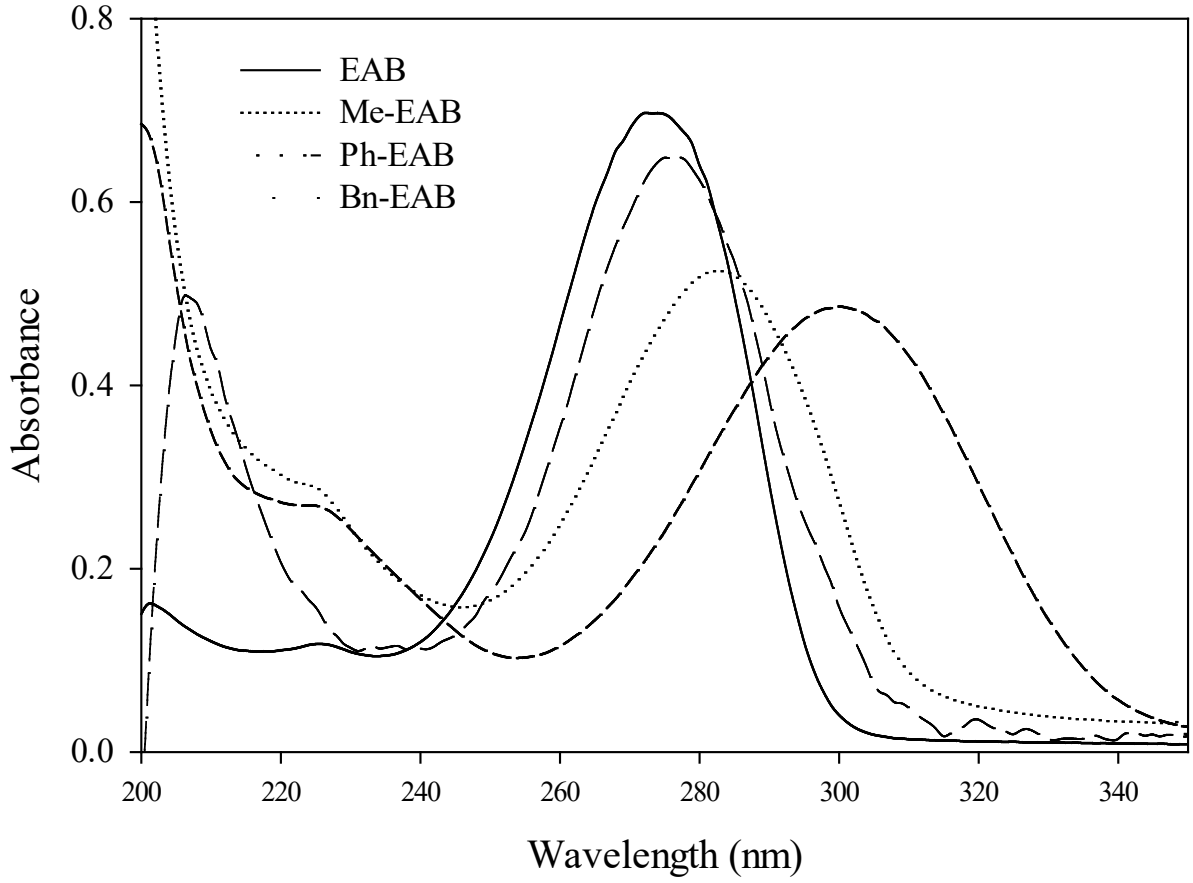
EAB
Me-EAB
Ph-EAB
Bn-EAB
Absorbance
Wavelength (nm)
0.0
0.2
0.4
0.6
0.8
200
220
240
260
280
300
320
340

Fig. S5.

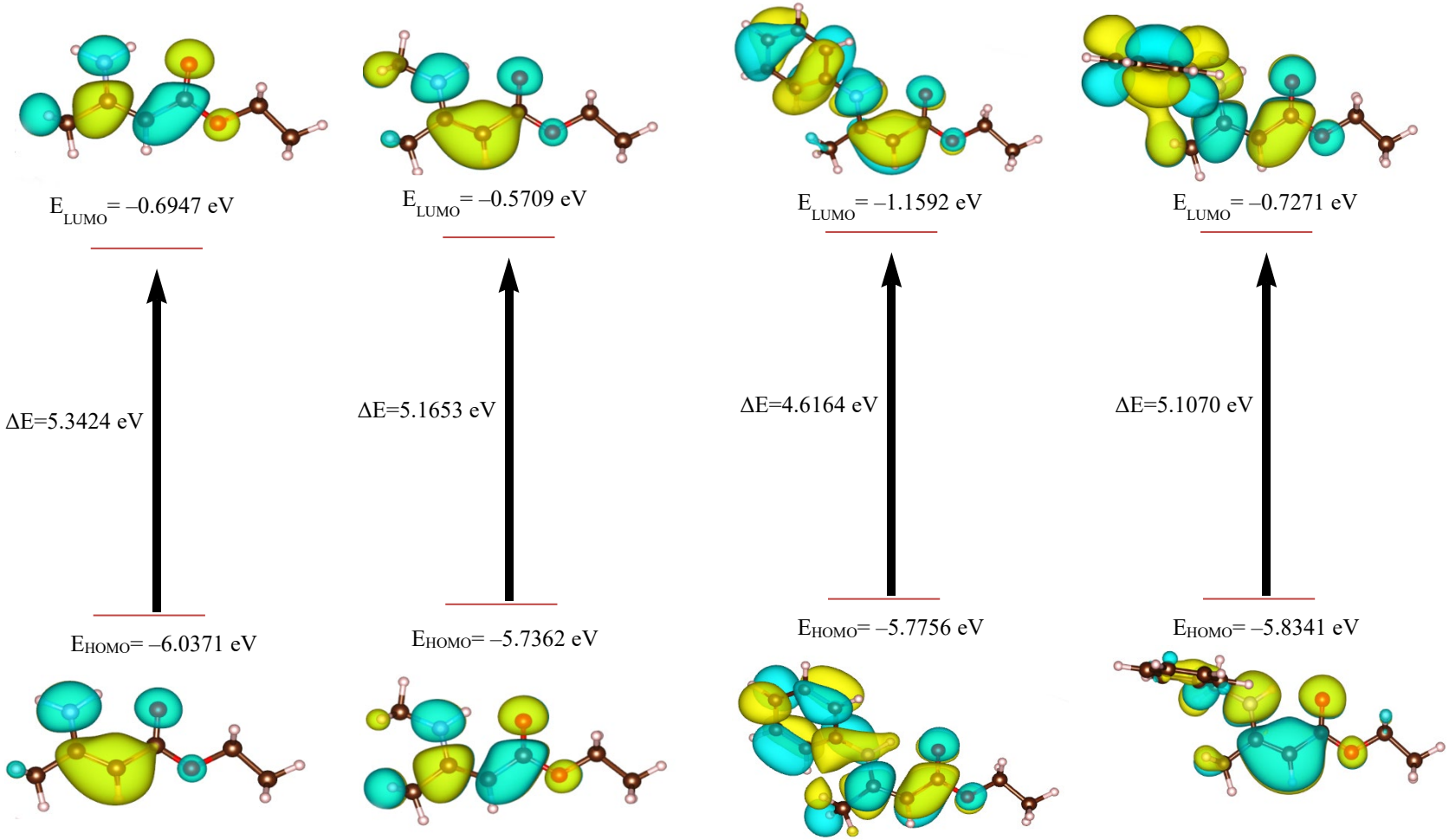
E LUMO = –0.6947 eV
E LUMO = –0.5709 eV
E LUMO = –1.1592 eV
E LUMO = –0.7271 eV
ΔE=5.3424 eV
ΔE=5.1653 eV
ΔE=4.6164 eV
ΔE=5.1070 eV
E HOMO = –6.0371 eV
E HOMO = –5.7362 eV
E HOMO = –5.7756 eV
E HOMO = –5.8341 eV

Fig. S6.

-5.174e -2 5.174e-2

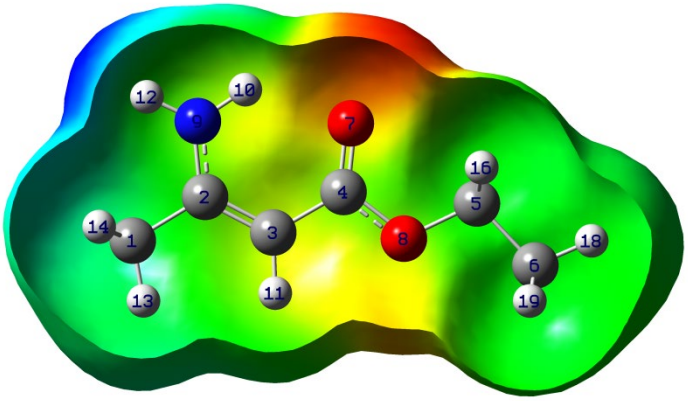

	Charges (e)	Electric Potential (a.u)
C1	-0.6079	-14.760
C2	0.2722	-14.712
C3	-0.4437	-14.794
C4	0.7720	-14.665
C5	-0.0321	-14.726
C6	-0.5880	-14.783
O7	-0.6784	-22.405
O8	-0.5679	-22.346
N9	-0.7731	-18.375
H10	0.4319	-1.029
H11	0.2204	-1.115
H12	0.3802	-1.016

-7.131e -2 7.131e-2

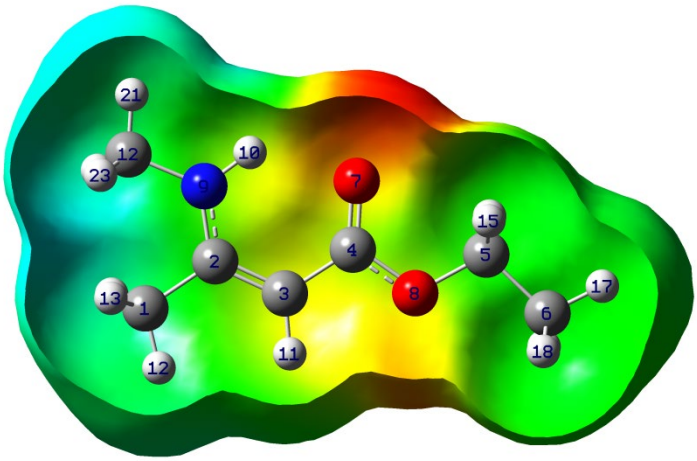

	Charges (e)	Electric Potential (a.u)
C1	-0.6116	-14.762
C2	0.2905	-14.716
C3	-0.4483	-14.799
C4	0.7691	-14.670
C5	-0.0316	-14.728
C6	-0.5877	-14.785
O7	-0.6873	-22.408
O8	-0.5695	-22.350
N5	-0.6072	-18.372
H10	0.4331	-1.036
H11	0.2190	-1.120
C12	-0.3612	-14.730

-6.750e -2 6.750e-2

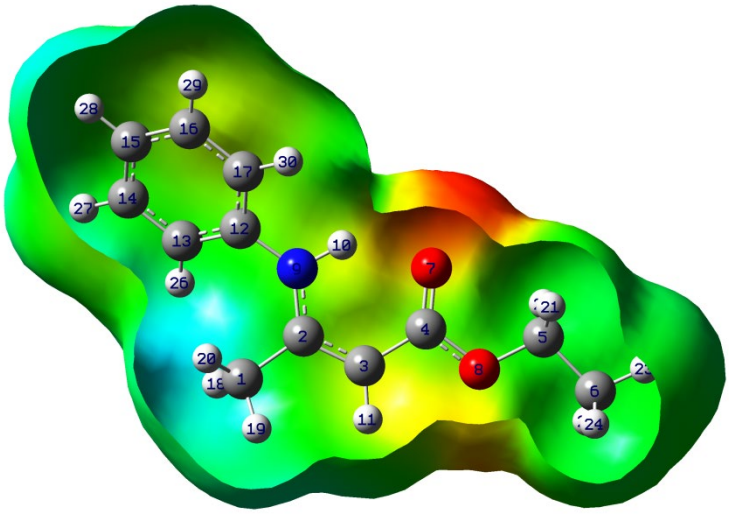

	Charges (e)	Electric Potential (a.u)
C1	-0.6127	-14.761
C2	0.2910	-14.707
C3	-0.4310	-14.790
C4	0.7709	-14.661
C5	-0.0322	-14.723
C6	-0.5883	-14.781
O7	-0.6892	-22.400
O8	-0.5648	-22.342
N9	-0.5979	-18.361
H10	0.4385	-1.026
H11	0.2209	-1.112
C12	0.1554	-14.719

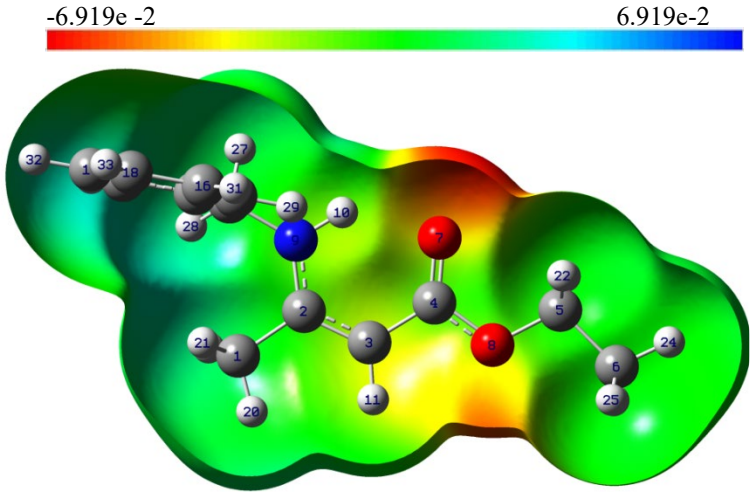

	Charges (e)	Electric Potential (a.u)
C1	-0.6156	-14.764
C2	0.2938	-14.714
C3	-0.4450	-14.797
C4	0.7699	-14.667
C5	-0.0318	-14.726
C6	-0.5878	-14.783
O7	-0.6854	-22.405
O8	-0.5679	-22.348
N9	-0.6130	-18.372
H10	0.4341	-1.035
H11	0.2200	-1.118
C12	-0.1887	-14.720

Figure S7.

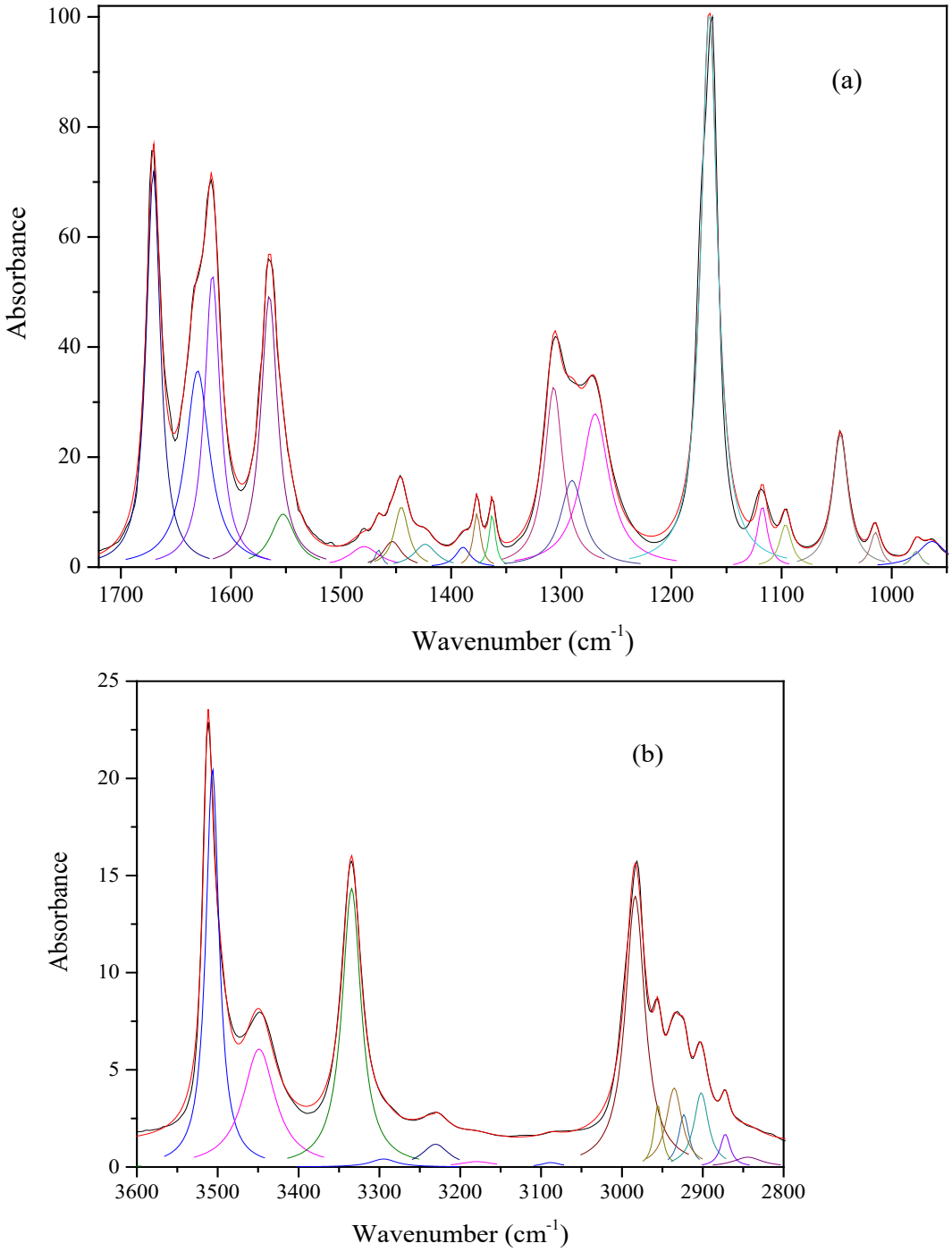

Fig. S8.

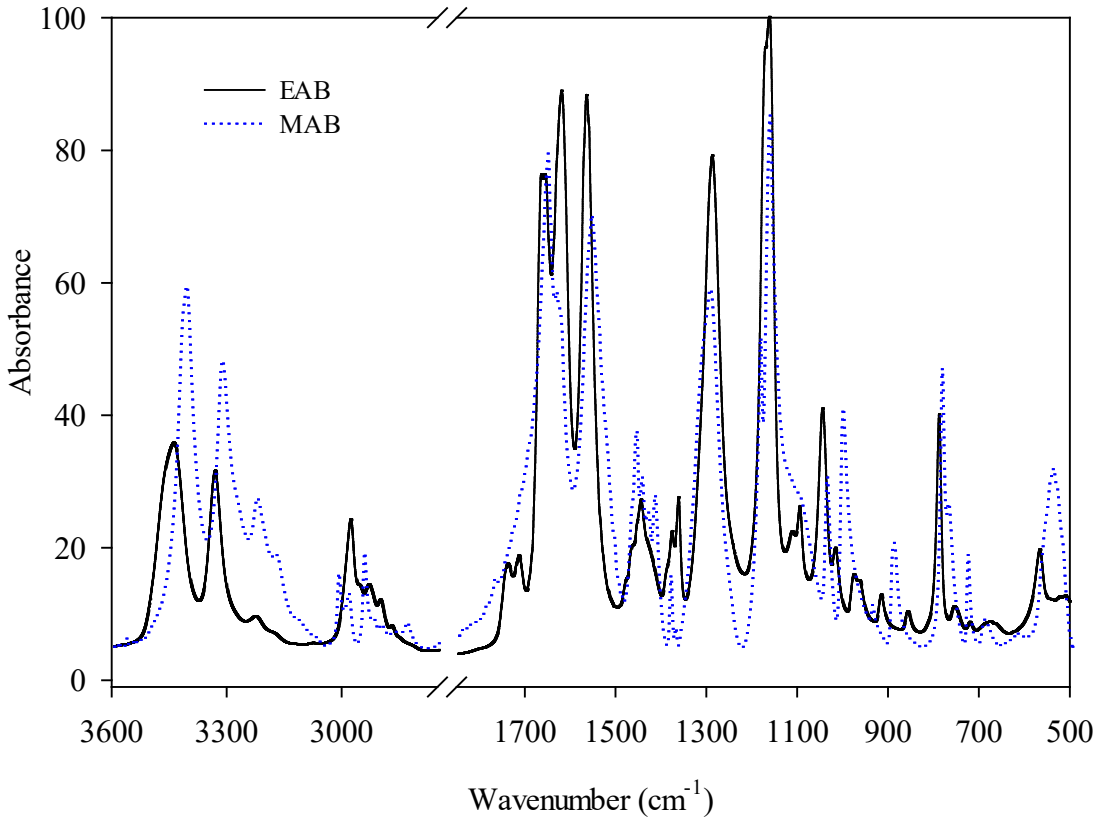
EAB
MAB
Absorbance
100
80
60
40
20
0
3600
3300
3000
1700
1500
1300
1100
900
700
500
Wavenumber (cm-1)

Fig. S9.

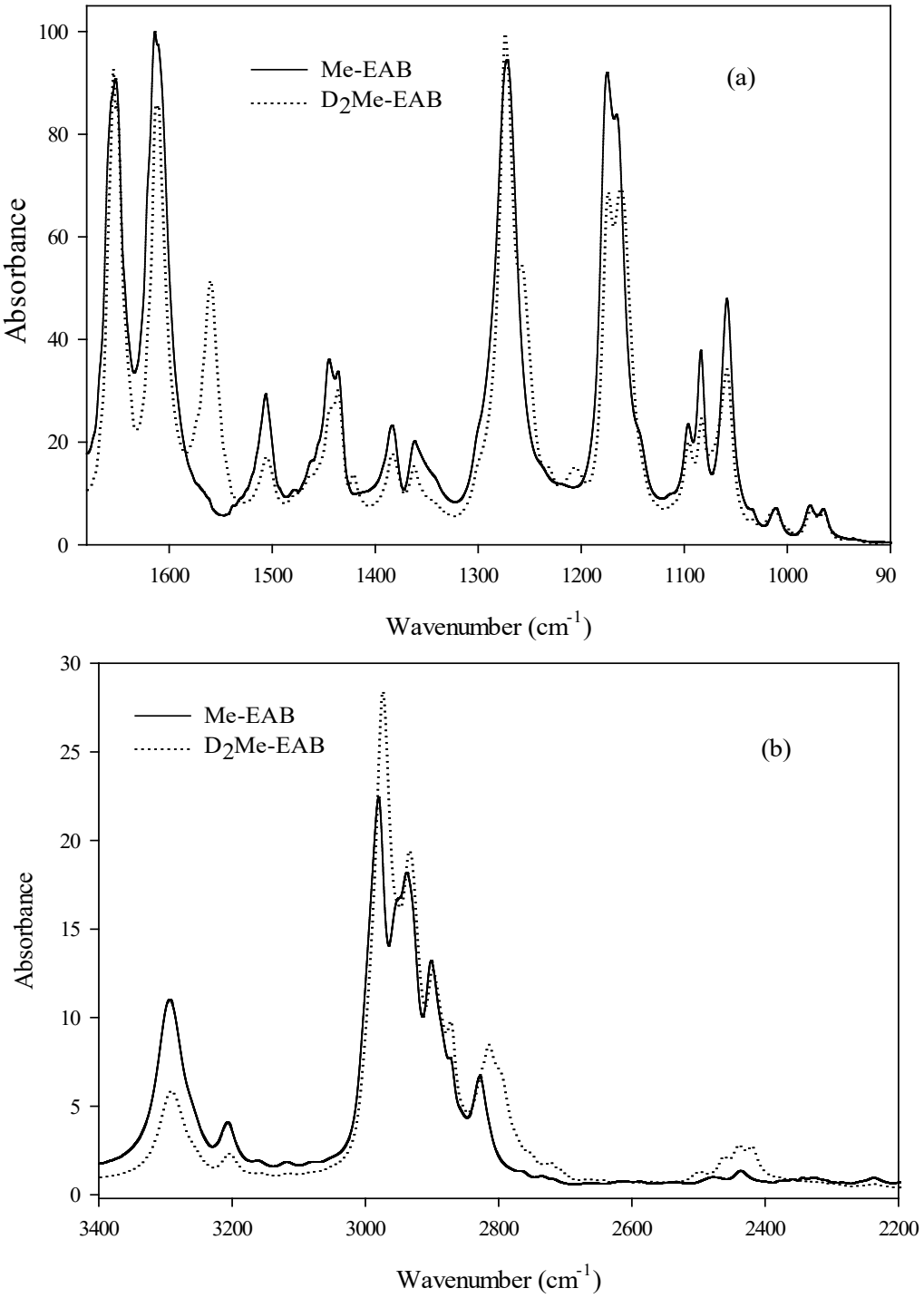
Me-EAB
D2Me-EAB
(a)
Absorbance
Wavenumber (cm-1)
Me-EAB
D2Me-EAB
(b)
Absorbance
Wavenumber (cm-1)

Fig. S10.

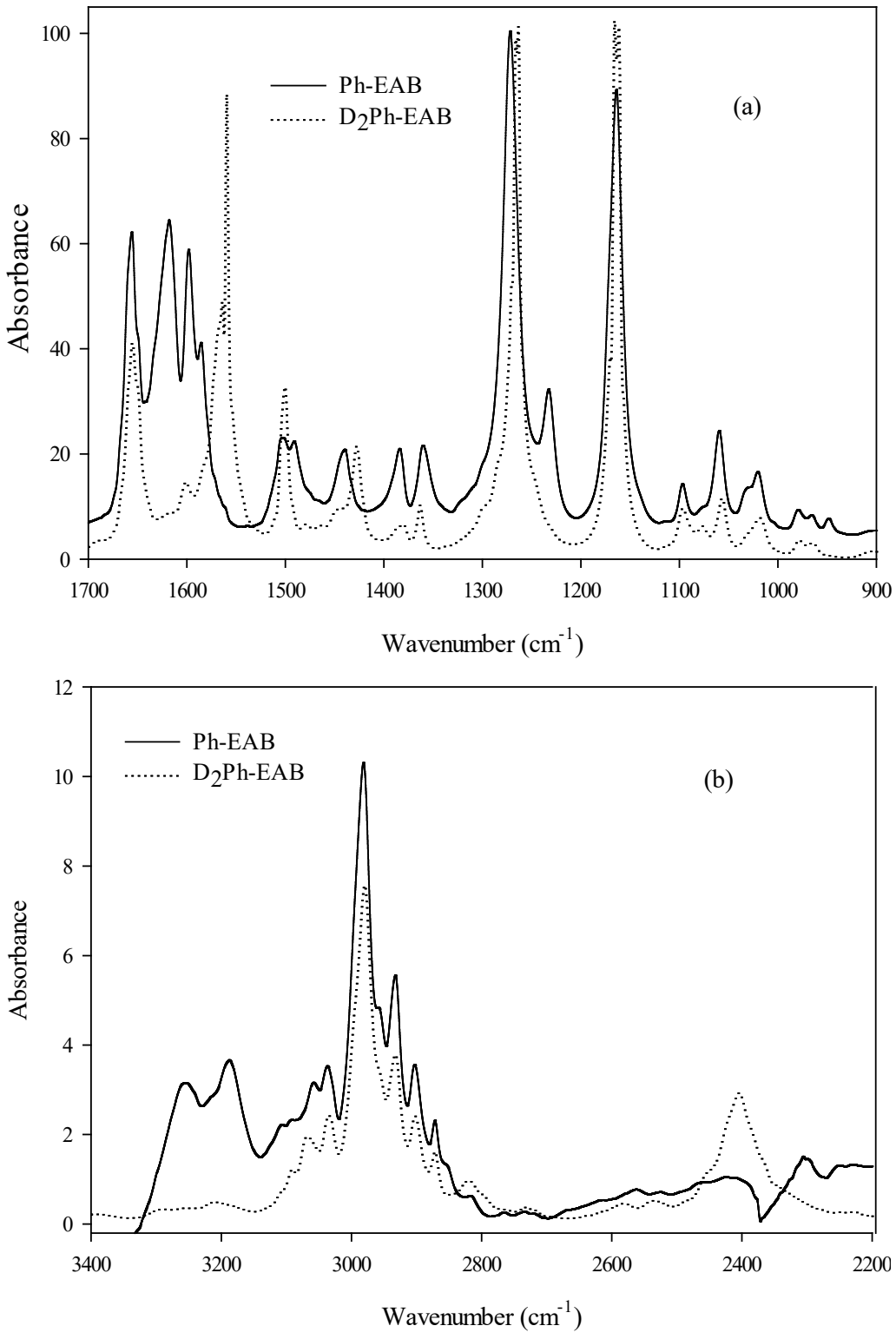
Ph-EAB
D2Ph-EAB
(a)
Absorbance
Wavenumber (cm-1)
Ph-EAB
D2Ph-EAB
(b)
Absorbance
Wavenumber (cm-1)

Fig. S11.

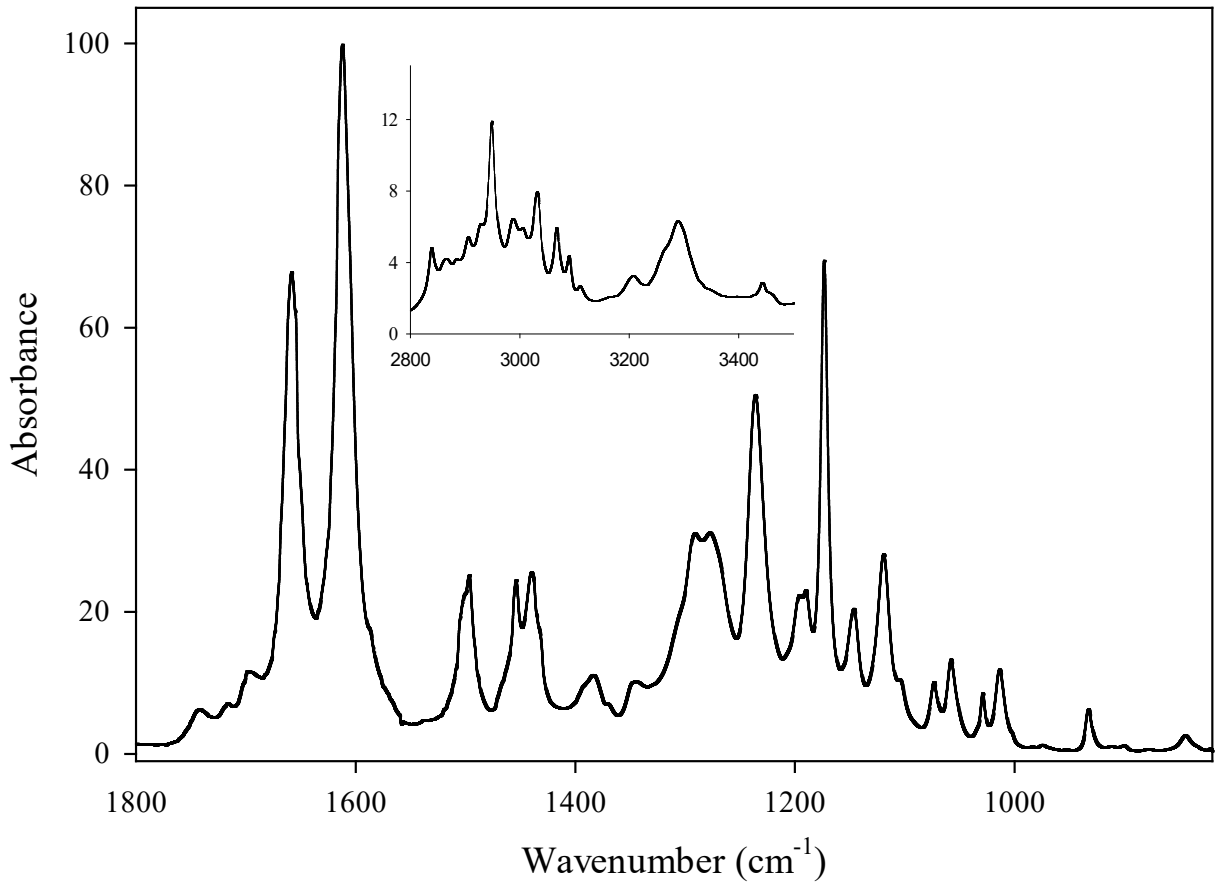
100
80
60
40
20
0
Absorbance
1800
1600
1400
1200
1000
Wavenumber (cm-1)
12
8
4
0
2800
3000
3200
3400

Fig. S12.